

MICROCOPY RESOLUTION TEST CHART  
NATIONAL BUREAU OF STANDARDS-1963-A

2

Contract N00014-81-K-0650

MECHANICS OF NEAR TIP MICROCRACKING  
IN BRITTLE MATERIAL

P. Charalambides and R. M. McMeeking  
Department of Theoretical and Applied Mechanics  
University of Illinois at Urbana-Champaign

March 1985

DTIC  
ELECTE  
JUN 5 1985  
S B D

DISTRIBUTION STATEMENT A  
Approved for public release  
Distribution Unlimited

85 04 22 026

64

AD-A154 684

DTIC FILE COPY

SUMMARY

A continuum mechanics description, of the phenomenon of stress induced microcracking has been used to study the near tip stress and strain fields and the size and shape of a small scale damaged zone for a stationary mode I crack in an elastic body. The material model is characterized by a microcracking criterion, which is an extension and simplification of the generalized microcracking criterion proposed by Fu and Evans [10] for the case of thermal stress-induced microcracking. That together with approximate expressions relating the effective composite moduli to the elastic properties of the brittle material, via the microcrack density  $\epsilon$  first introduced by Budiansky and O'Connell [1], yield a self consistent approach to the stress induced microcracking phenomenon.

The microcrack density was found to characterize three regions of interest. In the outer region the microcrack density is zero and the stress and strain fields are purely those for linear elastic deformation. This elastic field constrains the microcracking deformation which in combination with material weakening due to microcracking causes stress relaxation in a region of intermediate microcracking. Very close to the crack tip the microcrack density is saturated and the stress field becomes again singular but with a lower stress intensity than would prevail in the absence of microcracking. In the case where very rapid microcracking occurs as the strain is increased, the intermediate microcracking zone is still present providing continuity of the strain field and a smooth transition of the stress field from the purely elastic region to the region with saturated microcrack density. It appears that the existence of the region of intermediate microcrack density is essential to preserving the assumption of a continuum composite because it helps to avoid any strain and stress discontinuity.

INTRODUCTION

The self consistent approach to the stress-induced microcracking of brittle materials, as already mentioned, is based on two major notions. The notion of a microcracking criterion and that of effective elastic properties of the microcracked material. The microcracking criterion relates the induced microcrack density  $\epsilon$  to the existing stress magnitude. The effective elastic properties of the microcracked material are then functions of the initial elastic properties and the microcrack density. Budansky and O'Connell [1], introduced the microcrack density parameter  $\epsilon$  given by equation (1)

$$\epsilon = \frac{2N}{\pi} \left\langle \frac{A^2}{P} \right\rangle \quad (1)$$

where N=number of microcracks per unit volume, A is the area of the microcrack surface and P is the perimeter of the microcrack. Using energy balance considerations and fracture mechanics analysis they were able to derive mathematical expressions relating the effective elastic properties of the actual state to those of the unmicrocracked elastic state, through the microcracking density  $\epsilon$ . We will make use of the work of Fu and Evans [10] to construct a microcracking criterion which will relate increases in the microcracking density to increases in stress magnitudes. Together with the self consistent results of Budiansky and O'Connell [1], the microcracking criterion can be used to develop a constitutive law for the inelastic behavior of a microcracking continuum.

Our interest is in the development of microcracks near the tips of major cracks. To study this phenomenon in an approximate way, we use the constitutive law for the microcracking material in finite element calculations of either plane strain or plane stress deformation near the crack tip. These

**PER LETTER**



Dist	Special
A-1	

ides  
or

results are relevant to the question of microcrack toughening in brittle materials. Before we proceed to describe these results we will discuss briefly some previous work on this problem.

Hoagland, et al. [2], proposed a simplified method for estimating the density of microcracks in the vicinity of a major crack tip. They assume a set of randomly oriented lines, which are the traces of the potential microcrack planes, and which become microcracks when the stress normal to the line exceed a critical value. They also assume that the dimension of the microcracks is very much less than the major crack size of the model. In determining the stress intensity, they used the singular elastic stress field near the crack tip. Later studies done by Evans [3], suggest that the uniform microcrack density analysis presented by Hoagland et al. is inaccurate because there is an increased density of microcracks at the higher stress levels, which more strongly biases the microcrack density towards the crack tip.

In 1980 Hoagland and Embury [4], suggested a numerical procedure for modeling the number and distribution of microcracks around a crack tip, as a function of the applied stress intensity. The procedure accounts approximately for microcrack-microcrack and microcrack-crack interactions. This work is actually an extension of their original concept of nucleating microcracks based on a uniform fracture stress by adding new stress fields, whenever a new microcrack is nucleated. Although Hoagland and Embury arrived at some useful conclusions concerning the stress induced microcracking in the vicinity of a major crack, their results are restricted to a two-dimensional problem with through thickness microcracks extended along the third dimension. In contrast to that the theory developed by Budiansky and O'Connell accounts for microcracks with finite third dimension (i.e.,

circular, elliptical, etc.) and allows this effect to be introduced in an approximate way.

A more thorough investigation of the mechanics of microcrack toughening was carried out by Fu and Evans [10]. In their work they established the basis of a continuum mechanics description of the microcrack toughening process. The constitutive behavior of the microcrack zone is based on the overall strain response of a microcracking medium, subject to a uniform stress field. A generalized microcracking criterion for microcracking at facets subject to general stress is proposed. Stress induced microcracking is initiated at a threshold load. Above the threshold load, the stress/strain behavior becomes nonlinear. During unloading, linearity resumes and hysteresis is present, corresponding to dissipation of strain energy.

#### THE MICROCRACKING CRITERION AND CONSTITUTIVE LAW

Fu and Evans [10] studied the phenomenon of stress induced microcracking of grain boundary facets. These facets are generally subject to residual stresses caused by thermal expansion anisotropy of the neighboring grains. When a high tensile stress is applied, favorably oriented facets crack. The crack is confined to that facet and it takes a much higher stress to cause it to propagate out of its initial grain boundary interface. As a consequence, the process of microcracking is at least initially stable, with a steadily increasing stress causing the nucleation of more cracks rather than the propagation of existing ones.

From experiments and fracture mechanics analysis, Fu and Evans concluded that a particular facet will crack if it is larger than a critical size which depends on the resolved applied stress and the residual stress on the interface. In this notion is implicit the idea that facets can microcrack due

to the residual stress alone if the facet exceeds a critical size. Fu and Evans were able to phrase their results in terms of a parameter  $\epsilon$  introduced by Budiansky and O'Connell [1] to describe microcrack density. When there are  $N$  circular microcracks per unit volume and the microcracks are of uniform size with radius  $a$  then  $\epsilon = Na^3$ . Fu and Evans studied microcracking due to macroscopically uniform biaxial stress fields (with principal stresses  $\sigma_1 > \sigma_2$ ,  $\sigma_1 > 0$ ,  $k = \sigma_2/\sigma_1$ ). From their analysis and observations, they proposed

$$\epsilon = \lambda(\sigma)(\sigma_1 - \sigma_C) \quad \text{for } \sigma_1 > \sigma_C \quad (2)$$

where  $\lambda$  is a parameter that depends on stress state and material properties but independent of stress magnitude. For example  $\lambda$  for  $k=1$  is twice the value of  $\lambda$  for  $k=0$ . The parameter  $\epsilon$  represents the density of microcracks introduced by the applied stress that is in excess of any initial density. Thus the microcrack density  $\epsilon$  increases linearly with stress and does so up to a saturation level, after which it remains constant.  $\epsilon$  is unchanged by a reduction of stress.

We require a criterion for microcracking which can be used in more general states of multiaxial stress. For this purpose we will modify equation (2) to become.

$$\epsilon = \lambda(\sigma_R - \sigma_C) \quad \text{if } \sigma_R > \sigma_C \quad (3)$$

where  $\sigma_R = \sqrt{\sigma_{ij}\sigma_{ij}}$  is an effective stress,  $\sigma_C$  is the critical stress for microcracking initiation and  $\lambda$  is a material constant independent of stress state. Of course equation (3) only applies when the largest principal stress is tensile and increases monotonically. The criterion (3) is somewhat different from that proposed by Fu and Evans [10]. If we take the uniaxial

stress case with  $\sigma_1 = \sigma$  as a datum then both criteria give  $\epsilon = \lambda_u(\sigma - \sigma_C)$  where  $\lambda_u$  is the value of  $\lambda$  from Fu and Evans theory for uniaxial tension. For equal biaxial tension ( $\sigma_1 = \sigma_2 = \sigma$ ), Fu and Evans' criterion gives  $\epsilon = 2\lambda_u(\sigma - \sigma_C)$  whereas the one we have proposed leads to  $\epsilon = \lambda_u(\sqrt{2}\sigma - \sigma_C)$ . Thus our criterion shows a reduced rate of microcracking in biaxial tension compared to the rate suggested by Fu and Evans but microcracking starts at a lower stress according to our criterion. It can be argued that the microcrack density in biaxial tension would not be double that for uniaxial stress, since a given facet cannot be cracked twice. That is, unless the families of facets cracked by each applied stress component are mutually exclusive. However we are interested mainly in a simple constitutive law with appropriate characteristics for microcracking to illustrate what will occur near major crack tips. We will develop more exact microcracking laws in future work.

We summarize our microcracking criterion as follows.

For monotonically increasing stress, if

- |   |   |
|---|---|
| $\sigma_R < \sigma_C$ then $\epsilon = 0$   | Material remains unmicrocracked                             |
| $\sigma_C < \sigma_R < \sigma_M$ then $\epsilon = \lambda(\sigma_R - \sigma_C)$   | The microcrack density is increasing linearly with $\sigma$ |
| $\sigma_R > \sigma_M$ then $\epsilon = \lambda(\sigma_M - \sigma_C) = \epsilon_M$ | The microcrack density is saturated.                        |
- (4)

Furthermore  $\epsilon$  cannot decrease. The stress/strain relation given for a macroscopic element of material is linear for non-microcracked regions ( $\epsilon=0$ ), becomes nonlinear for regions with increasing microcrack density  $0 < \epsilon < \epsilon_M$  and again becomes linear for fully microcracked regions ( $\epsilon = \epsilon_M$ ). During unloading linearity resumes and when material unloads to zero stress no permanent strains are present as shown in fig. (1).

It should be noted that the microcrack distribution produced by a deviatoric applied stress coupled with the residual stress will be anisotropic. However, Fu and Evans used the isotropic theory of Budiansky and O'Connell [1] to determine macroscopic moduli for the microcracked material. that is they used  $\epsilon$  as if it represented a random distribution of microcracks rather than an oriented one. We will follow Fu and Evans in this regard to obtain an approximate continuum theory for microcracking.

We have found that we can approximate Budiansky and O'Connell's results as follows.

$$\frac{\bar{E}}{E} = \frac{\bar{\nu}}{\nu} = 1 - \frac{16}{9} \epsilon = \frac{1}{f} \quad (5)$$

where  $E$ ,  $\nu$  and  $\bar{E}$ ,  $\bar{\nu}$  are Young's moduli and Poisson's ratio for the material before and after stress induced microcracking respectively. Note that  $\bar{E}$  and  $\bar{\nu}$  are defined at constant  $\epsilon$ . Thus the constitutive equation for the microcracking solid becomes

$$e_{ij} = \frac{f+\nu}{E} \sigma_{ij} - \frac{\nu}{E} \sigma_{kk} \delta_{ij} \quad (6)$$

where  $e$  is the macroscopic strain,  $\sigma$  is the macroscopic stress,  $\delta_{ij}$  is the kronecker delta and rules for  $f$  are given by equations (3), (4) and (5).

The constitutive equation (6) is only valid for values of the microcracking parameter  $f$  within the interval  $1 < f < \infty$ , fig (3). This together with equation (5) defines the limiting values of the microcracking density  $\epsilon$ ,  $0 < \epsilon < \frac{9}{16}$  (See fig (3)). The upper bound of  $\epsilon$  with the aid of equation (3) yield a relation between the critical stresses  $\sigma_C$ ,  $\sigma_M$  and the parameter  $\lambda$  i.e.,  $\sigma_M - \sigma_C < \frac{9}{16} \cdot \frac{1}{\lambda}$  (See fig (4)).

FORMULATION OF CRACK TIP PROBLEM

The high stresses near the tip of a long crack will cause microcracking in the near tip region in the material of interest to us, as shown in fig (5). We will restrict our attention to the situation where the zone of microcrack damage is very small compared to the body containing the crack. We will refer to this situation as small scale microcracking. In this case, the microcrack zone will lie within a region of uncracked material. some distance outside the zone, the stresses will be almost the same as when the material does not microcrack. When small scale microcracking prevails, these stresses will be the singular linear elastic crack tip stresses.

It follows that the plane small scale microcracking problem can be solved by considering a plane region around the crack tip to which are applied boundary tractions given by the linear elastic stress field, i.e.

$$T_i = n_j \sigma_{ij} = \frac{K_I}{\sqrt{2\pi r}} n_j \zeta_{ij}(\theta) \quad (7)$$

where  $T_i$  are the boundary tractions,  $n_j$  is the outward unit normal to the region boundary,  $K_I$  is the mode I (tensile opening mode) stress intensity factor and  $(r, \theta)$  are polar coordinates originating at the crack tip as shown in fig (6). The function  $\zeta_{ij}$  determines the angular distribution of stress and its form can be found in the article by Rice [23]. The crack surfaces are traction free. To ensure small scale microcracking,  $K_I$  must be limited to a level low enough that the zone size is small compared to the region for which the analysis is being carried out

The governing equations of equilibrium and compatibility are enforced through the principle of virtual work

$$\int_A \sigma_{ij} \delta e_{ij} dA = \int_{S_T} T_i \delta u_i ds \quad (8)$$

In the absence of body forces, where A is the plane area being analyzed,  $S_T$  is the perimeter where tractions are prescribed,  $u$  are the displacements and the symbol  $\delta$  indicates a virtual variation of the quantity following it and the variation disappears on  $S - S_T$ .

The constitutive law for the material has been described in the previous section. However, we will find it useful to state the following form.

$$\sigma_{ij} = c_{ijkl} e_{kl} = \frac{E}{f+v} e_{ij} + \frac{E \cdot v}{(f-2v)(f+v)} e_{kk} \delta_{ij} \quad (9)$$

where  $f = \frac{1}{1 - \frac{16}{9} \epsilon}$  and  $\epsilon = \epsilon(\sigma)$  as in equation (3)

For plane problems

$$e_{\alpha\beta} = \frac{f+v}{E} [\sigma_{\alpha\beta} - v^* \sigma_{\gamma\gamma} \delta_{\alpha\beta}] \quad \alpha, \beta, \gamma = 1, 2 \quad (10\alpha)$$

$$\sigma_{\alpha\beta} = \frac{E}{f+v} [e_{\alpha\beta} + \frac{v^*}{(1-2v^*)} e_{\gamma\gamma} \delta_{\alpha\beta}] \quad (10\beta)$$

where  $v^* = \frac{v}{f}$  for plane strain and  $v^* = \frac{v}{f+v}$  for plane stress. The governing equations, together with the appropriate boundary conditions corresponding to a specified geometry, define a boundary value problem whose solution we will obtain numerically.

#### THE FINITE ELEMENT EQUATIONS

The finite element equations can be derived from the principle of virtual work given by equation (8). Finite element interpolations together with

equation (8) and the constitutive law (9) and (10.β), give rise to the nonlinear finite element equations

$$[k(u_n)]\{u_n\} = \{F\} \quad (11)$$

where  $[k]$  is the stiffness matrix,  $\{u_n\}$  the nodal displacement vector and  $\{F\}$  the force vector. The notation  $[k(u_n)]$  indicates the dependence of the stiffness on the nodal displacements due to the nonlinear constitutive law.

In the finite element analysis, a 4 noded quadrilateral isoparametric element with 4 stations for the integration of stiffness was used. The finite element equations (11) were solved using an iterative method updating the stiffness matrix in every iteration. The microcracking parameter  $f$  was found to be the root of a sixth order polynomial in  $f$  which satisfies the conditions imposed on  $f$  earlier in this work i.e.  $1 < f < \infty$ . The coefficients of the polynomial are strain dependent and had to be recomputed in every iteration [see Appendix II].

To ensure small scale microcracking, the outer radius of the mesh was chosen to be 15 to 20 times the outer radius of a damaged zone, estimated from the stresses in the absence of microcracking.

## RESULTS

### Stress-strain fields

Figs (7) to (8) display the stresses and strains ahead of the crack tip for various choices of  $\lambda$  and  $\epsilon_M$ .  $\lambda$  is the rate of increase of the microcrack density with respect to the effective stress and  $\epsilon_M = \lambda(\sigma_M - \sigma_c)$  is the saturation value of the microcrack density.

In the unmicrocracked region, both stresses and strains agree quite closely with the solution obtained for an unmicrocracked material. The elastic strain and stress fields constrain the deformation due to

microcracking in the damaged zone. The above constraint together with the weakening of the material in the damaged zone due to microcracking, causes stress relaxation in the region of intermediate microcracking. Very close to the crack tip the microcracking density is saturated and the stress and strain fields become singular again. We observe that the amount of stress relaxation increases with  $\lambda$  and it reaches its maximum level for  $\lambda = \infty$ . At this point we notice the importance of the presence of the zone of intermediate microcracking, for its presence ensures a smooth transition for both the strain and stress fields from the outer to the inner asymptotic fields. The absence of the above region would lead to infinite strain and stress gradients along the boundary of the fully microcracked material and the unmicrocracked material [see Appendix I]. We also notice that in the stress relaxation region, the effective stress which in our case is the equivalent stress

$\sigma_R = \sqrt{\sigma_{ij} \sigma_{ij}}$  is consistent with the microcracking law eq (3), fig (2) that we used. In the particular case of  $\lambda = \infty$ ,  $\sigma_R = \sigma_c = 1.0$  as we expected. In this situation, the partially microcracked zone is like a perfectly plastic zone. The zone with saturated microcrack density is dominated by microcracking deformation with larger strains and stresses at lower levels than would prevail in the absence of microcracking.

#### The shape and size of the transformed zone

A typical microcrack zone is shown in fig. (5). Three characteristic quantities describing the microcrack zones that we studied were consistently computed.  $x_m$  is the distance along the x axis at which the microcrack zone boundary crosses the x axis.  $h_m$  denotes the y coordinate of the farthest point along the y direction to experience microcracking and  $\theta_m$  is the polar angle corresponding to the same point. The boundary of the inner zone, where

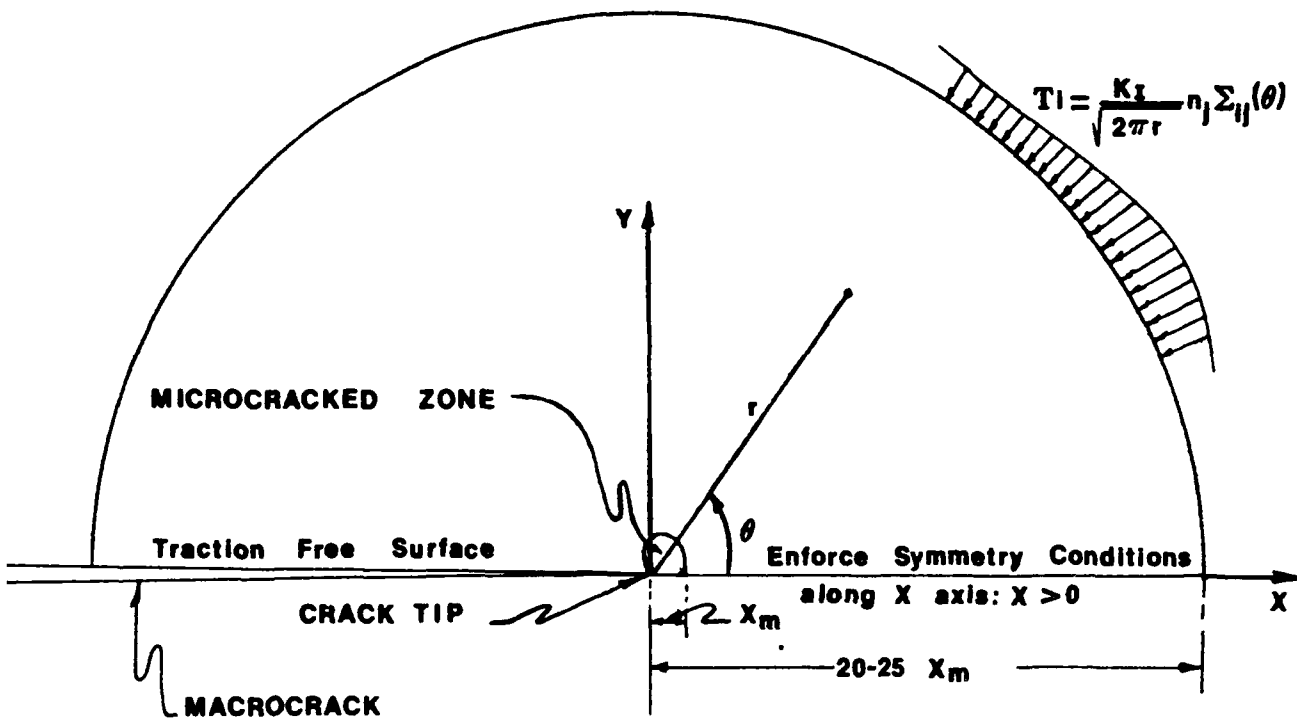


**Fig. 6 The BOUNDARY CONDITIONS used in solving the FINITE ELEMENT equations**

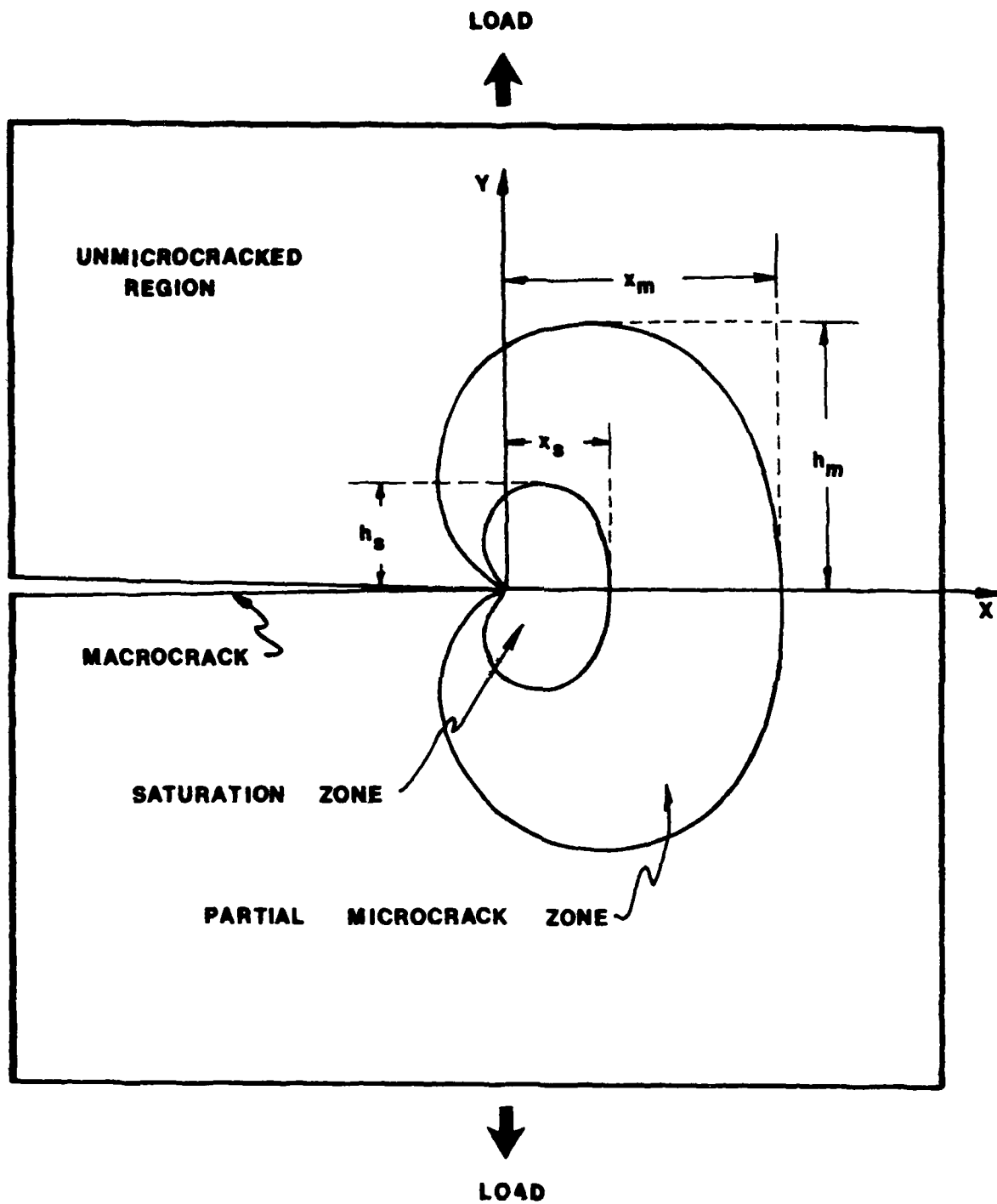


Fig. 5 Microcracking at the vicinity of the crack tip of a semi-infinite macrocrack under mode I Loading

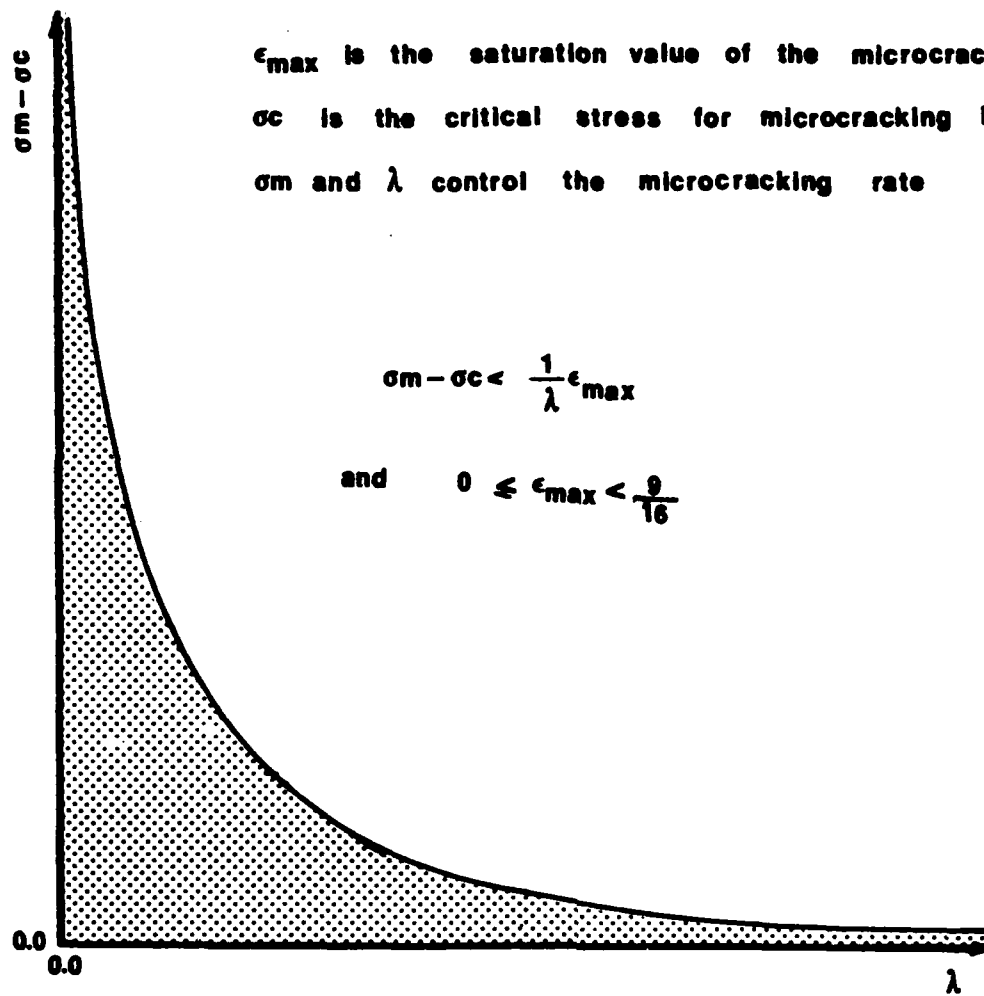
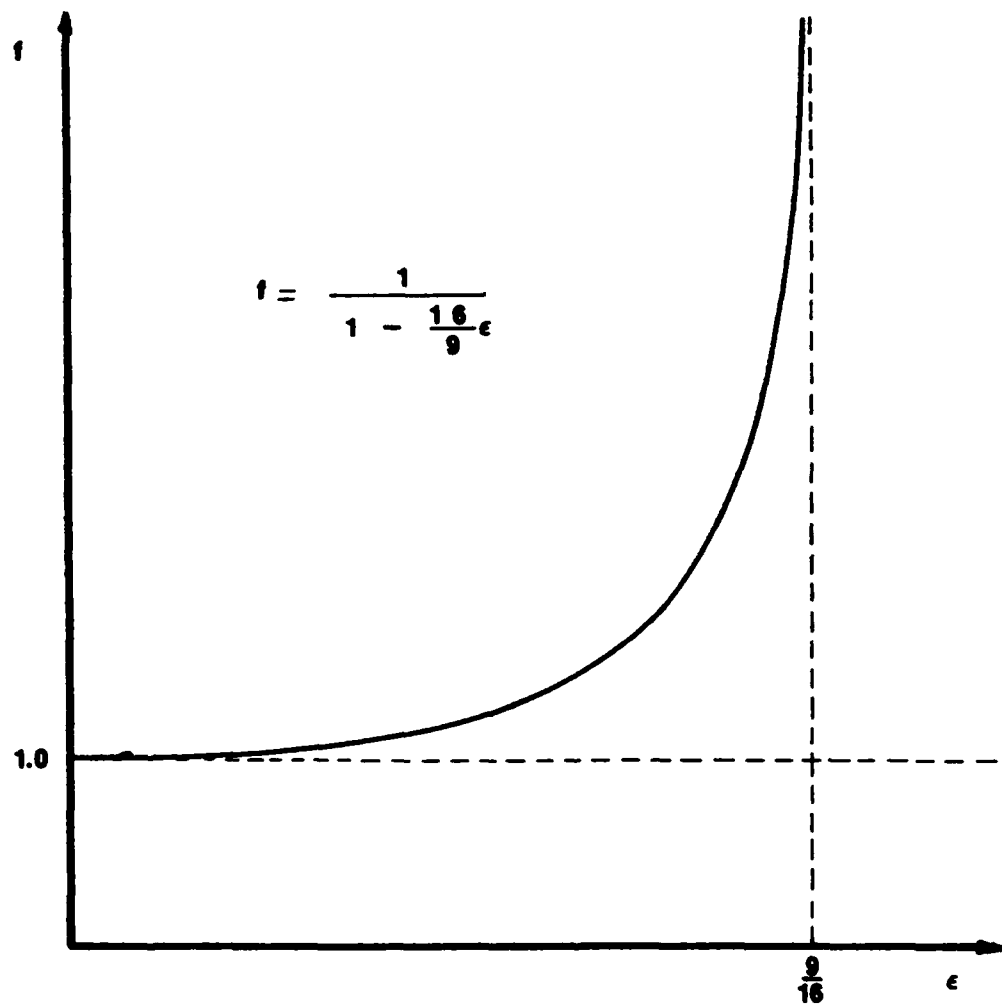


Fig. 4 Relations between the constants  $\epsilon_{\max}$ ,  $\sigma_c$ ,  $\sigma_m$  and  $\lambda$



**Fig. 3** Microcracking parameter  $f$  versus microcracking density  $\epsilon$

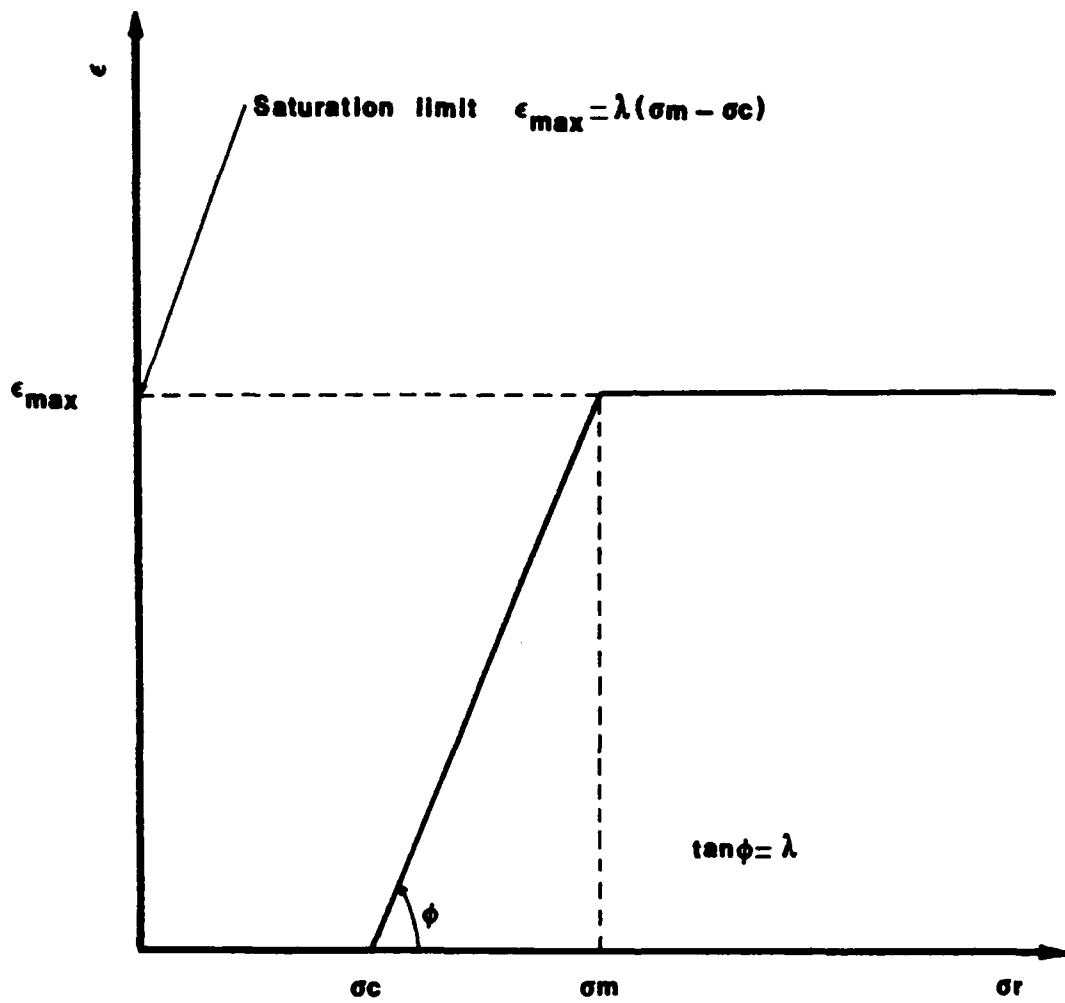
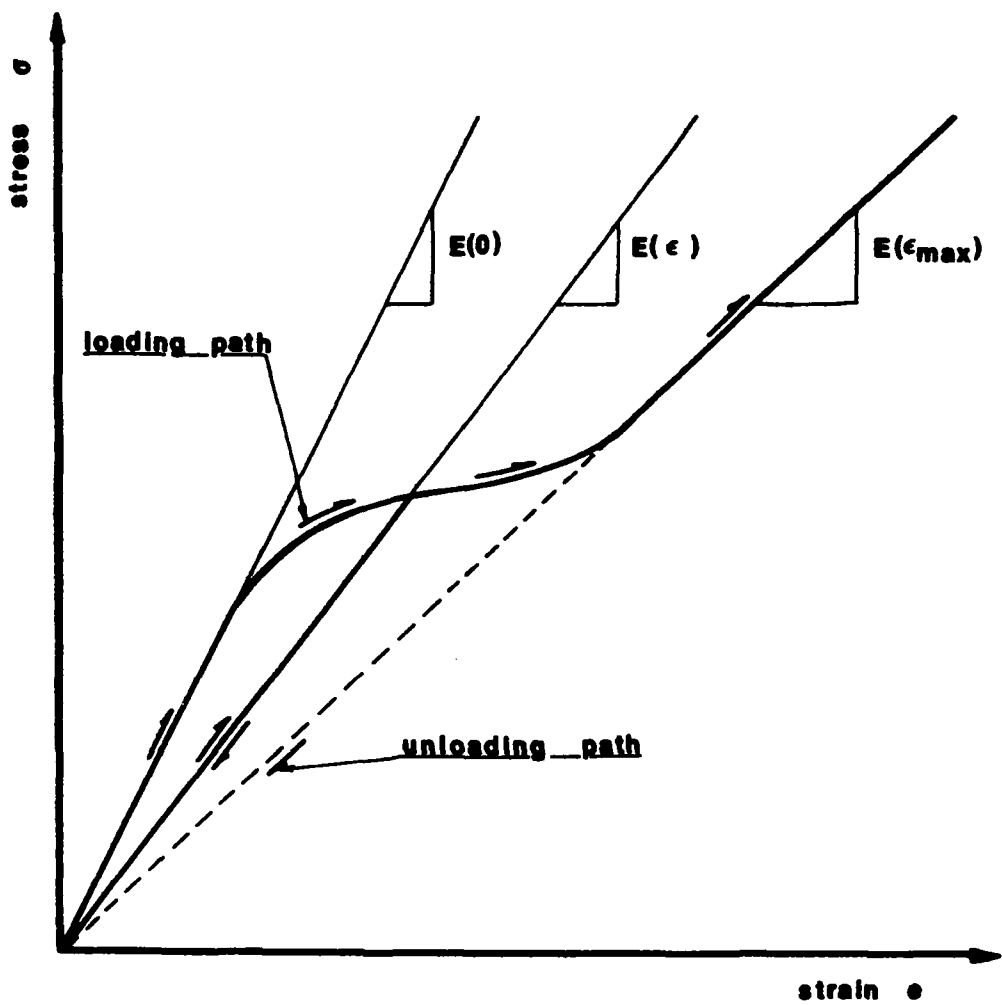


Fig. 2 Microcracking density  $\epsilon$  versus equivalent stress  $\sigma$



**Fig.1** Stress-Strain curve for a microcracked material

References

1. B. Budiansky and R. J. O'Connell. "Elastic moduli of Cracked Solid" Int. J. Solids Structures Vol. 12, 81-97 (1975).
2. R. G. Hoagland, J. D. Embury and D. J. Green. "On the density of microcracks formed during the fracture of ceramics" Scr. Metall., 9, 9, 907 (1975).
3. A. G. Evans "On the formation of a crack tip microcrack zone." Scr. Metall. 10, 1, 93-97 (1976).
4. R. G. Hoagland and J. D. Embury. "A treatment of inelastic deformation around a crack tip due to microcracking" J. Am. Ceram. Soc, 63, 7, 404 (1980).
5. Y. Fu and A. G. Evans. "Microcrack zone formation in single phase polycrystals" Acta Metal. Vol 30, 1619-1625 (1982).
6. R. M. McMeeking and A. G. Evans. "Mechanics of Transformation Toughening in Brittle materials." J. Amer. Ceram. Soc. 65(5), 242-245 (1982).
7. B. Budiansky, J. W. Hutchinson and J. C. Lampropoulos, "Continuum theory of dilatant transformation toughening in Ceramics." Int. J. Solids Structures Vol 19, 337-355, (1983).
8. A. G. Evans and K. T. Faber. "Crack-growth resistance of Microcracking Brittle Materials." J. Amer. Ceram. Soc. 67, 4, 255-260 (1983).
9. K. T. Faber "Microcracking Contributions to the toughness of ZrO<sub>2</sub>-Based Ceramics.. To appear in Advances in ceramics 11: Pceedings of the second International conference on the science and technology of Zirconia.
10. Yen Fu, "Mechanics of microcracking toughening in ceramics" Ph.D. Thesis U.C.B.C. (1983).
11. Rice, J. R. "Mathematical Analysis in the Mechanics of Fracture" in Fracture, An Advanced Treatise (Ed. H. Liebowitz) Academic Press, 192-308 (1968).

$$\text{let } \alpha = \lambda \sigma_C + \frac{9}{16}$$

$$\beta = \lambda \sigma_C \cdot \nu + \frac{9}{16} (\nu - 1)$$

$$\gamma = -\frac{9}{16} \cdot \nu$$

then for plane strain:

$$a_6 = \alpha^2$$

$$a_5 = 2\alpha\beta - 4\nu\alpha^2$$

$$a_4 = \beta^2 + 2\alpha\gamma - 8\nu\alpha\beta + 4\nu^2\alpha^2 - \lambda^2 E^2 [e_x^2 + e_y^2 + \frac{1}{2} \gamma_{xy}^2]$$

$$a_3 = 2\beta\gamma - 4\nu(\beta^2 + 2\alpha\gamma) + 8\alpha\beta\nu^2 - 2\lambda^2 E^2 \nu [(e_x + e_y)^2 - 2\nu[e_x^2 + e_y^2 + \frac{1}{2} \gamma_{xy}^2]] \quad (8)$$

$$a_2 = \gamma^2 - 8\nu\beta\gamma + (\beta^2 + 2\alpha\gamma)4\nu^2 - (\lambda E \nu)^2 [4(e_x^2 + e_y^2 + \frac{1}{2} \gamma_{xy}^2) - (e_x + e_y)^2]$$

$$a_1 = 8\beta\gamma\nu^2 - 4\nu\gamma^2$$

$$a_0 = 4\nu^2\gamma^2$$

for plane stress

$$a_6 = \alpha^2$$

$$a_5 = 2\alpha\beta - 2\nu\alpha^2$$

$$a_4 = \beta^2 + 2\alpha\gamma - 4\nu\alpha\beta + \nu^2\alpha^2 - \lambda^2 E^2 [e_x^2 + e_y^2 + \frac{1}{2} \gamma_{xy}^2]$$

$$a_3 = 2\beta\gamma - 2\nu(\beta^2 + 2\alpha\gamma) + 2\alpha\beta\nu^2 - \lambda^2 E^2 \nu [4e_x e_y - \gamma_{xy}^2] \quad (9)$$

$$a_2 = \gamma^2 - 4\beta\gamma\nu + \nu^2(\beta^2 + 2\alpha\gamma) - (\lambda E \nu)^2 [e_x^2 + e_y^2 + \frac{1}{2} \gamma_{xy}^2]$$

$$a_1 = 2\beta\gamma\nu^2 - 2\nu\gamma^2$$

$$a_0 = \nu^2\gamma^2$$

APPENDIX II

The microcracking law given by equation (3) earlier in this paper allow us to determine the microcrack density  $\epsilon$  for a given stress state. It is more convenient to determine  $\epsilon$  or  $f = 1/(1 - \frac{16}{9} \epsilon)$  for a given strain state.

from the constitutive law 
$$\sigma_{ij} = \frac{E}{f+v} [e_{ij} + \frac{v}{f-2v} e_{kk} \delta_{ij}] \quad (1)$$

we get 
$$\sigma_R = [\sigma_{ij} \sigma_{ij}]^{1/2} = \frac{E}{f+v} [e_{ij} e_{ij} + v \frac{2f-v}{(f-2v)^2} e_{kk}^2]^{1/2} \quad (2)$$

then we have the following cases in computing f.

i)  $\sigma_R(f) < \sigma_C \Rightarrow \epsilon = 0 \Rightarrow f = \frac{1}{1 - \frac{16}{9} \epsilon} = 1. \quad (3)$

ii)  $\sigma_R(f) > \sigma_M \Rightarrow \epsilon = \epsilon_M = \lambda(\sigma_M - \sigma_C) \Rightarrow f = \frac{1}{1 - \frac{16}{9} \epsilon_M} \quad (4)$

iii)  $\sigma_C < \sigma_R(f) < \sigma_M \Rightarrow \epsilon = \lambda(\sigma_R - \sigma_C). \quad (5)$

substituting  $\sigma_R$  from equation (2) in eqn (5) we have

$$\frac{9}{16} (1 - \frac{1}{f}) = \lambda \frac{E}{f+v} [e_{ij} e_{ij} + v \frac{2f-v}{(f-2v)^2} e_{kk}^2]^{1/2} - \lambda \sigma_C. \quad (6)$$

which is a sixth order polynomial in f of the form

$$a_6 f^6 + a_5 f^5 + a_4 f^4 + a_3 f^3 + a_2 f^2 + a_1 f + a_0 = 0 \quad (7)$$

whose coefficients are given below.

stress discontinuity

we allow  $\bar{\sigma}_{xx} = \sigma_{xx}$  and require  $\bar{e}_{yy} = e_{yy}$

we get  $(f+v)(1-\bar{v}^*)\bar{\sigma}_{yy} = (1-\bar{v}^*)\sigma_{yy} + (\bar{v}^*(f+v) - \bar{v}^*(1+v))\sigma_{xx}$

or  $\bar{\sigma}_{yy} = \frac{1}{f} \sigma_{yy}$  for Plane stress

and  $\bar{\sigma}_{yy} = f \frac{1-\bar{v}^2}{f^2-\bar{v}^2} \sigma_{yy} - (f-1) \frac{\bar{v}^2}{f^2-\bar{v}^2} \sigma_{xx}$  for Plane strain

strain discontinuity

we allow  $\bar{e}_{yy} = e_{yy}$  and require  $\bar{\sigma}_{xx} = \sigma_{xx}$

we get  $\bar{e}_{xx} = \left[ \frac{\bar{v}^*}{1-\bar{v}^*} \frac{(f+v)(1-2\bar{v}^*)}{(1-\bar{v})(1-2\bar{v}^*)} - \frac{\bar{v}^*}{1-\bar{v}^*} \right] e_{yy} - \frac{1-\bar{v}^*}{1-\bar{v}^*} \frac{(f+v)(1-2\bar{v}^*)}{(1-\bar{v})(1-2\bar{v}^*)} e_{xx}$

Plane strain:  $\bar{e}_{xx} = \left( \frac{f-2\bar{v}}{(1-2\bar{v})(1-\bar{v})} - \frac{1}{f-\bar{v}} \right) \bar{v} e_{yy} + \frac{1-\bar{v}}{f-\bar{v}} \frac{(f-\bar{v})(f-2\bar{v})}{(1-\bar{v})(1-2\bar{v})} e_{xx}$

Plane stress:  $\bar{e}_{xx} = \frac{\bar{v}}{f} \left( \frac{f^2-1}{1-\bar{v}} e_{yy} + \frac{1}{f} \frac{f+v}{1+\bar{v}} e_{xx} \right)$

Notice that for  $f=1$  (unmicrocracked material)  $\bar{\sigma}_y = \sigma_y$  and  $\bar{e}_{xx} = e_{xx}$ , both stress and strains are continuous. for microcracked materials  $f>1$  and  $\bar{\sigma}_y < \sigma_y$  whereas  $\bar{e}_{xx} > e_{xx}$ . The strains are larger in the microcracked region and the stresses fall to a lower value.

APPENDIX I

We consider an element consisting of two dissimilar material



$E, \nu$  are the Young modulus and Poisson's ratio for an unmicrocracked material.

$\bar{E}, \bar{\nu}$  are the corresponding moduli for a microcracked material.

We require that the material remains continuous after deformation. Thus from equilibrium and compatibility we get the interface conditions

$$\left. \begin{aligned} \bar{\sigma}_{xx} &= \sigma_{xx} \\ \bar{e}_{yy} &= e_{yy} \\ \bar{\sigma}_{xy} &= \sigma_{xy} = 0 \end{aligned} \right\} \text{interface conditions.}$$

The constitutive relations for plane elasticity case are

unmicrocracked solid

$$e_{\alpha\beta} = \frac{H\nu}{E} (\sigma_{\alpha\beta} - \nu^* \sigma_{\gamma\gamma} \delta_{\alpha\beta}) \quad \nu^* = \nu \quad \text{Plane strain}$$

$$\sigma_{\alpha\beta} = \frac{E}{1+\nu} (e_{\alpha\beta} + \frac{\nu^*}{(1-2\nu^*)} e_{\gamma\gamma} \delta_{\alpha\beta}) \quad \nu^* = \frac{\nu}{1+\nu} \quad \text{Plane stress}$$

microcracked solid

$$\bar{e}_{\alpha\beta} = \frac{f+\nu}{E} (\bar{\sigma}_{\alpha\beta} - \bar{\nu}^* \bar{\sigma}_{\gamma\gamma} \delta_{\alpha\beta}) \quad \bar{\nu}^* = \frac{\nu}{f} \quad \text{Plane strain}$$

$$\bar{\sigma}_{\alpha\beta} = \frac{E}{f+\nu} (\bar{e}_{\alpha\beta} + \frac{\bar{\nu}^*}{(1-2\bar{\nu}^*)} \bar{e}_{\gamma\gamma} \delta_{\alpha\beta}) \quad \bar{\nu}^* = \frac{\nu}{f+\nu} \quad \text{Plane stress}$$

where  $f = \frac{1}{1 - \frac{16}{9} \epsilon}$ , where  $\epsilon$  is the microcrack density.

The finite element analysis will substantially contribute to a better understanding of the mechanics of stress induced microcrack toughening in brittle material. As we saw earlier in our analysis, a zone with saturated microcrack density always exists. We may be able to treat this zone as being composed of homogeneous elastic material and use a Griffith criterion for propagation of the major crack into this zone. McMeeking, in unpublished work, has shown that the material obeying the constitutive law of eq. (3-6) is nonlinear hyperelastic. It follows that the J-integral is path independent throughout the material in both unmicrocracked and microcracked regions. As a consequence, the energy release rate for the microcracking material will have the same value as in the nonmicrocracking material at the same applied loads. Thus if the critical value for propagation is unchanged, then no microcrack toughening can occur. However, the critical energy release rate for fully microcracked material may differ from that for the unmicrocracked case. A simple model of the crack growing from microcrack facet to microcrack facet suggests that the average critical energy release rate would be less and so microcrack embrittlement would occur. However, aspects of R-curve type behavior and more realistic microcracking laws may hold the clue to microcrack toughening. Some of these issues have been addressed by Faber [9] and we will consider such issues in the future.

#### ACKNOWLEDGEMENT

This research was supported by the Office of Naval Research through Contract NR 064-N00014-81-K-0650 with the University of Illinois.

## DISCUSSION

Using the concept of the microcrack density  $\epsilon$  first introduced by Budiansky and O'Connell [1] together with a further simplified microcracking law proposed by Fu and Evans [10], we establish the basis of a continuum mechanics description for the phenomenon of stress-induced microcracking in a brittle polycrystalline composite. With appropriate integration of the constitutive relations we were able to obtain information as to what happens in the process zone at the vicinity of the crack tip of a major crack under a mode I loading in a material susceptible to microcracking. For appropriate choices of parameters, the transformation zone, as in the case of small scale yielding in a ductile material, is well contained. The stress and strain fields exhibiting the characteristics shown in fig (7) and (8) are well behaved. When the first critical stress  $\sigma_C$  and the saturation value  $\epsilon_M$  are specified, the second critical stress  $\sigma_M$  or the variable  $\lambda$  appearing in the microcracking law control the rate at which the material microcracks and affects the stress and strain fields as well as the shape and size of the transformation zone.

At this point, we have all the necessary tools for a full scale investigation of the phenomenon of microcracking. Such an investigation should address the question of the possible effects on material toughening due to microcracking. Further work is necessary to elucidate the nature of the crack propagation criterion. In addition studies done by McMeeking and Evans [6] and Budiansky et al. [7], suggest that the toughness of certain ceramics can be substantially enhanced through the controlled use of martensitic transformation. Faber [9] found that microcracking contributes to the toughness of  $ZrO_2$  - ceramics and Fu and Evans [10] found that stress induced microcracking enhances the toughness of brittle polycrystalline aggregates.

the microcrack density is saturated is also characterized by the corresponding quantities  $x_s$ ,  $h_s$  and  $\theta_s$  fig. (5).

Fig. (9) to fig (9 $\gamma$ ) show how the above quantities depend on the second critical stress  $\sigma_M$ , for fixed values of  $\sigma_c$  and  $\epsilon_M = \lambda(\sigma_M - \sigma_c)$ . The size of the fully microcracked zone is inversely proportional to the value of the second critical stress  $\sigma_M$ . Similarly high saturation values of the microcrack density yield small saturation zone. There is an increase in the size of the above zone in both directions as  $\lambda$  increases or  $\sigma_M$  decreases. In no case does the inner zone becomes identical with the whole damaged zone because as we said earlier the existences of a zone of intermediate microcracking is an essential feature of the microcracking law eq(3). The microcrack zone boundary depends on the first critical stress  $\sigma_c$ . For fixed values of both the first critical stress  $\sigma_c$  and the saturation microcrack density the microcrack boundary tends to stretch along the x axis while reduction of  $h_m$  is observed, as  $\lambda$  increases. The angles  $\theta_m$  and  $\theta_s$  corresponding to  $h_m$  and  $h_s$  drop from  $78^\circ$  for small values of  $\lambda$ , to  $49^\circ$  as  $\lambda$  becomes infinite. Fig (10) shows microcrack zones obtained through our finite element analysis. Fig (11) and (12) show the profile of the microcrack density ahead of the crack tip for various values of  $\sigma_M$ .

#### Plane stress results

Similar results to those of the plane strain case were obtained for the plane stress case. The transverse constraint of the plane strain case produces large transformation zones. the overall response of a microcracking material was found to be similar for both plane strain and plane stress cases.

Fig. 7  $\sigma_{xx}$  stress ahead of the crack tip

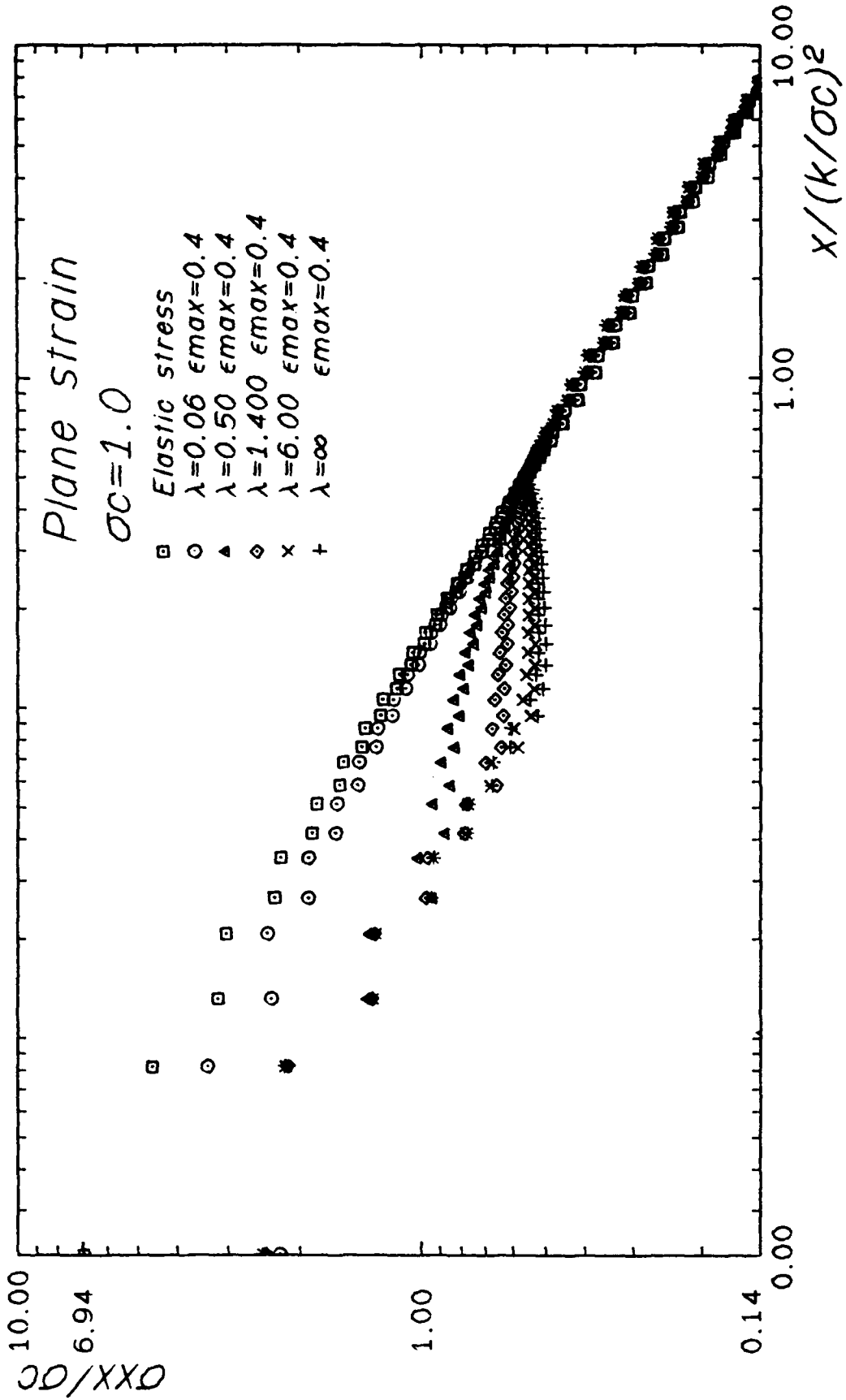


Fig. 7a  $\sigma_{yy}$  stress ahead of the crack tip

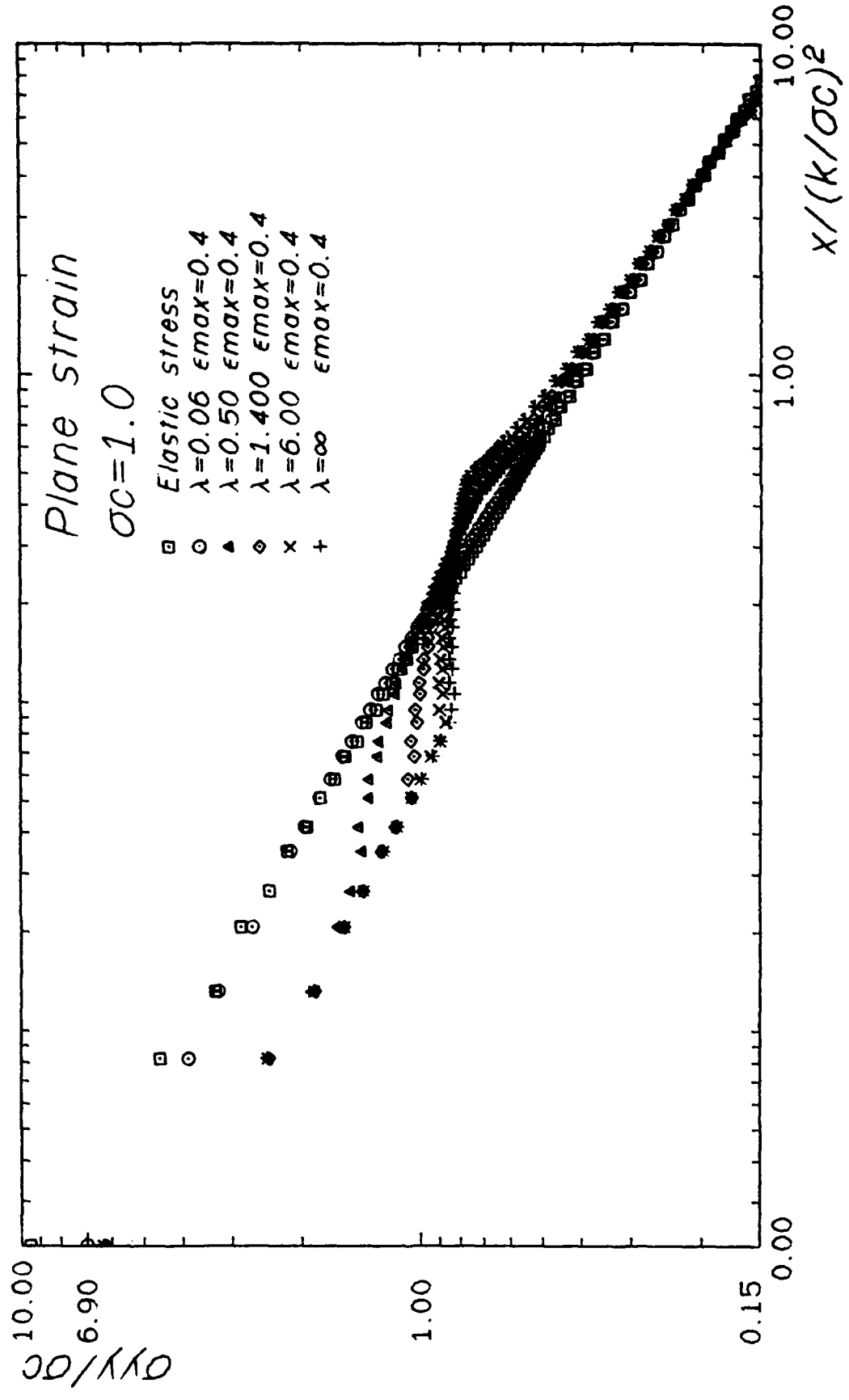


Fig. 7β Equivalent stress ahead of the crack tip

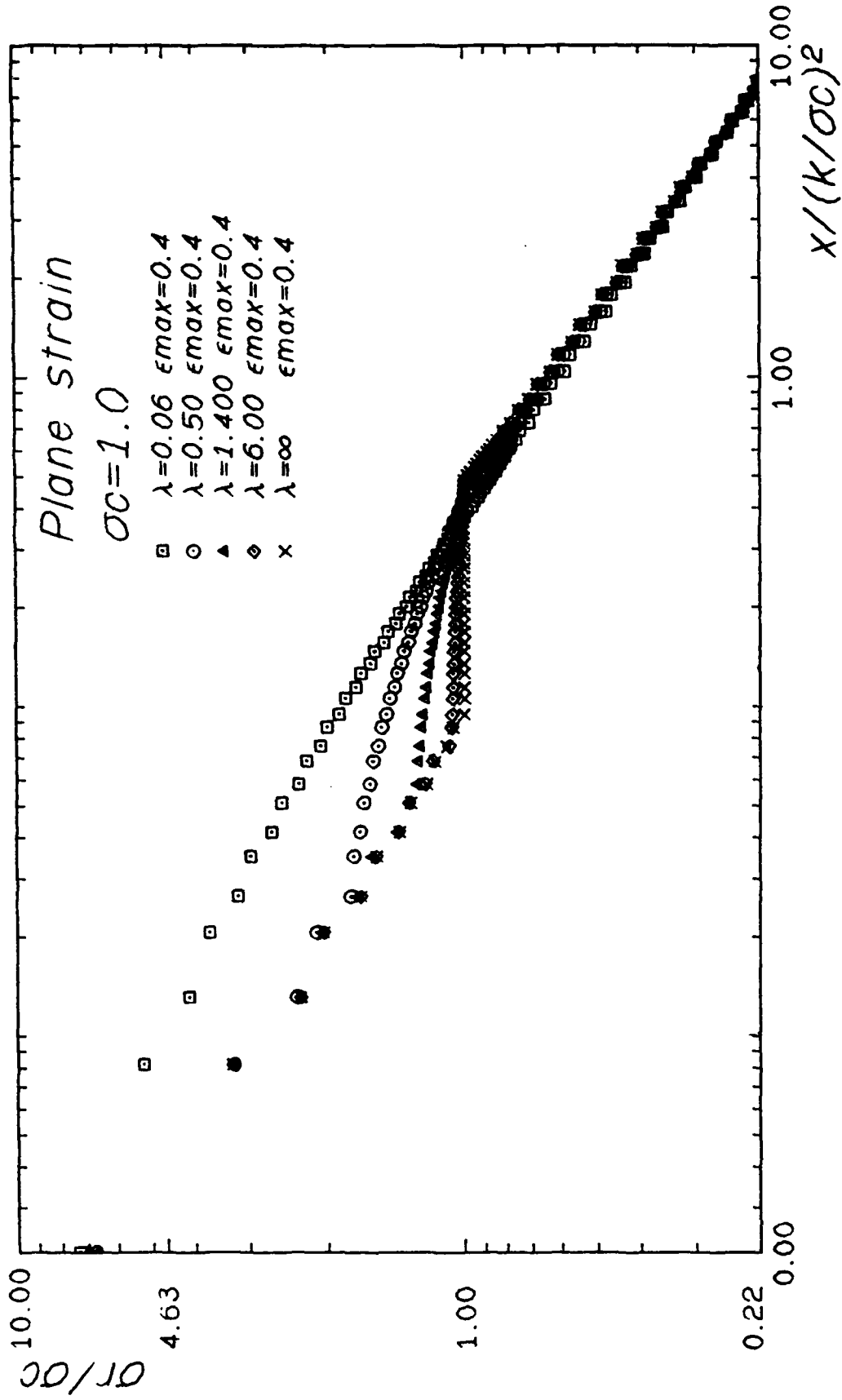


Fig. 8  $\epsilon_{xx}$  strain ahead of the crack tip

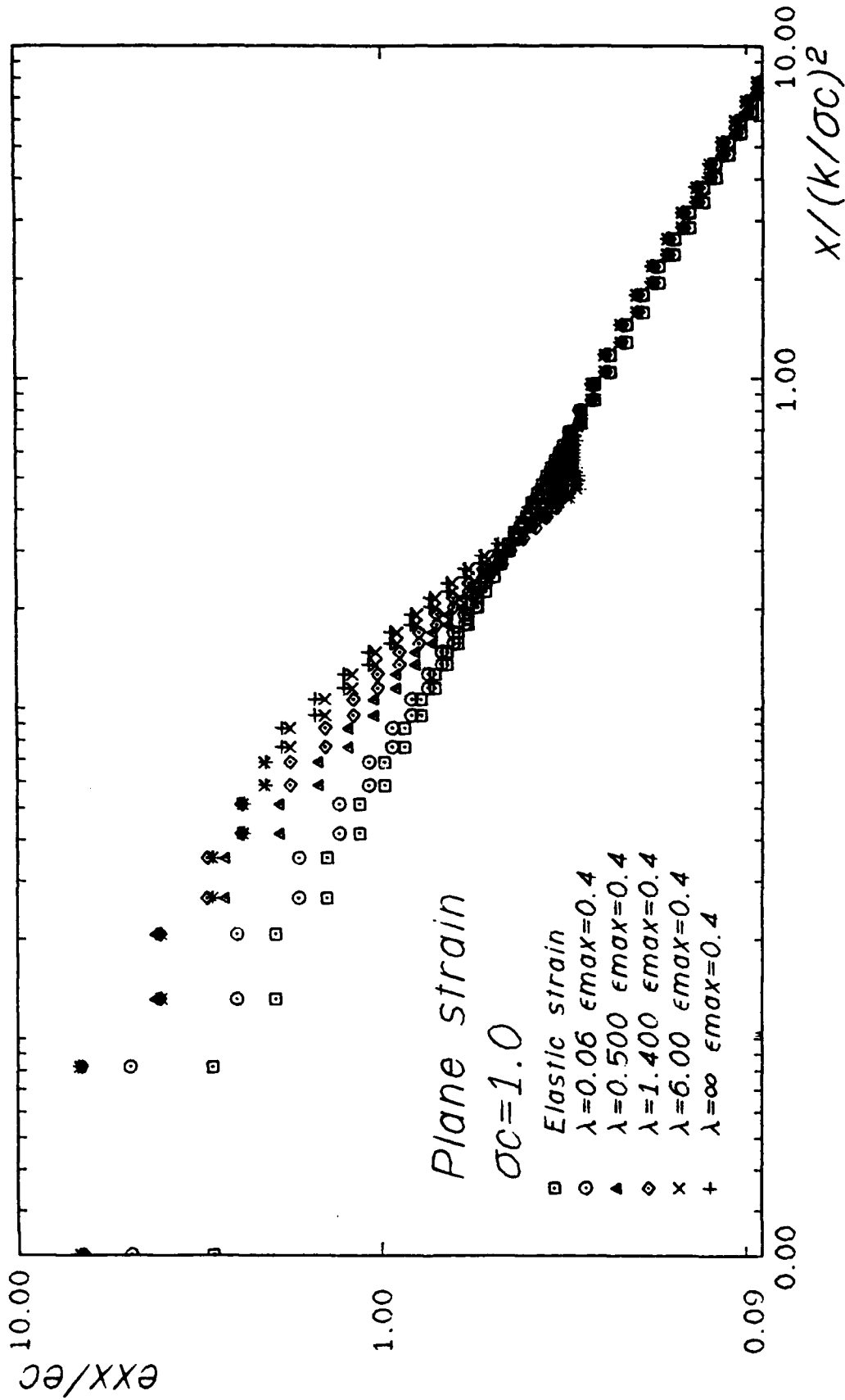
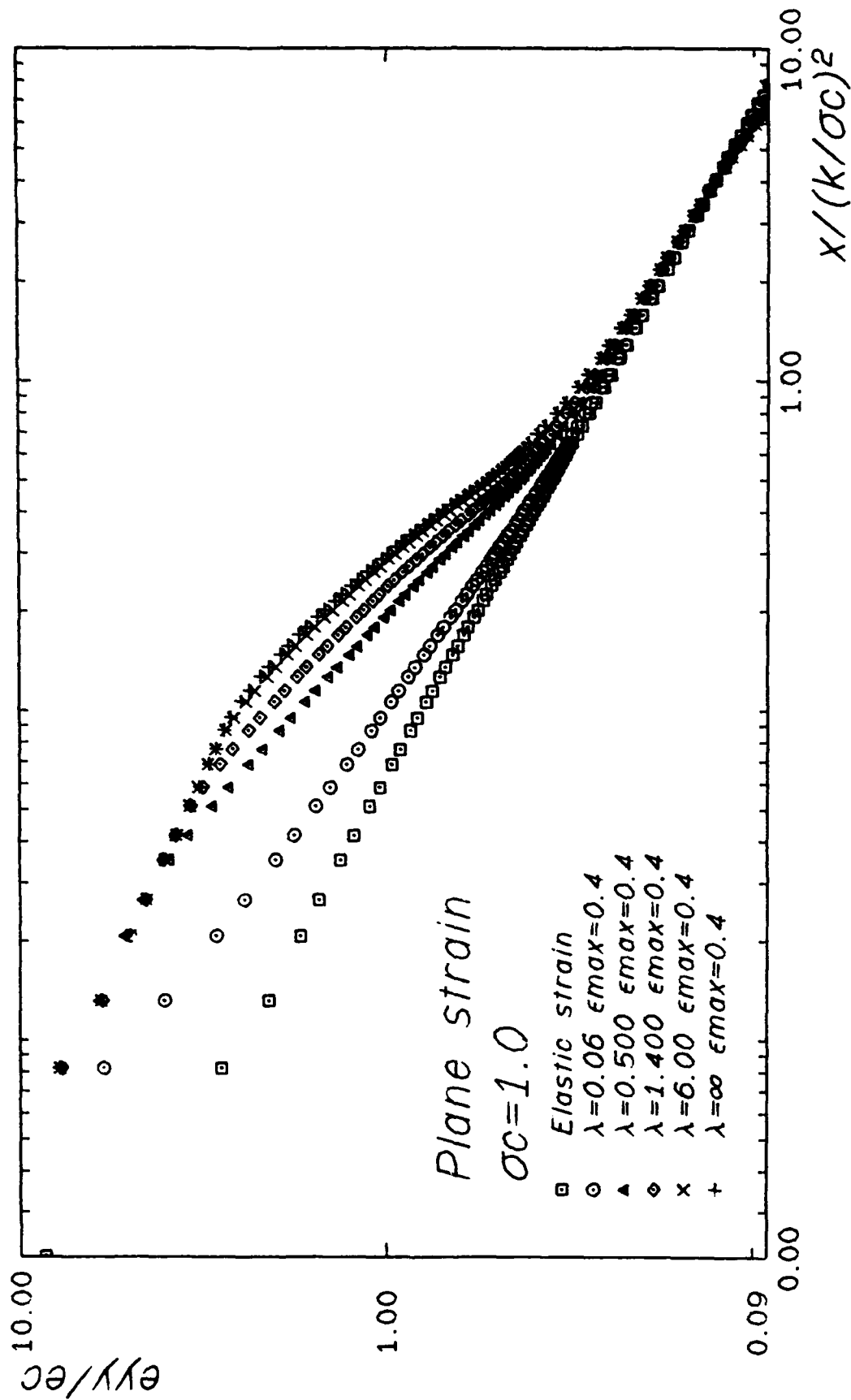


Fig. 8a  $\epsilon_{yy}$  strain ahead of the crack tip



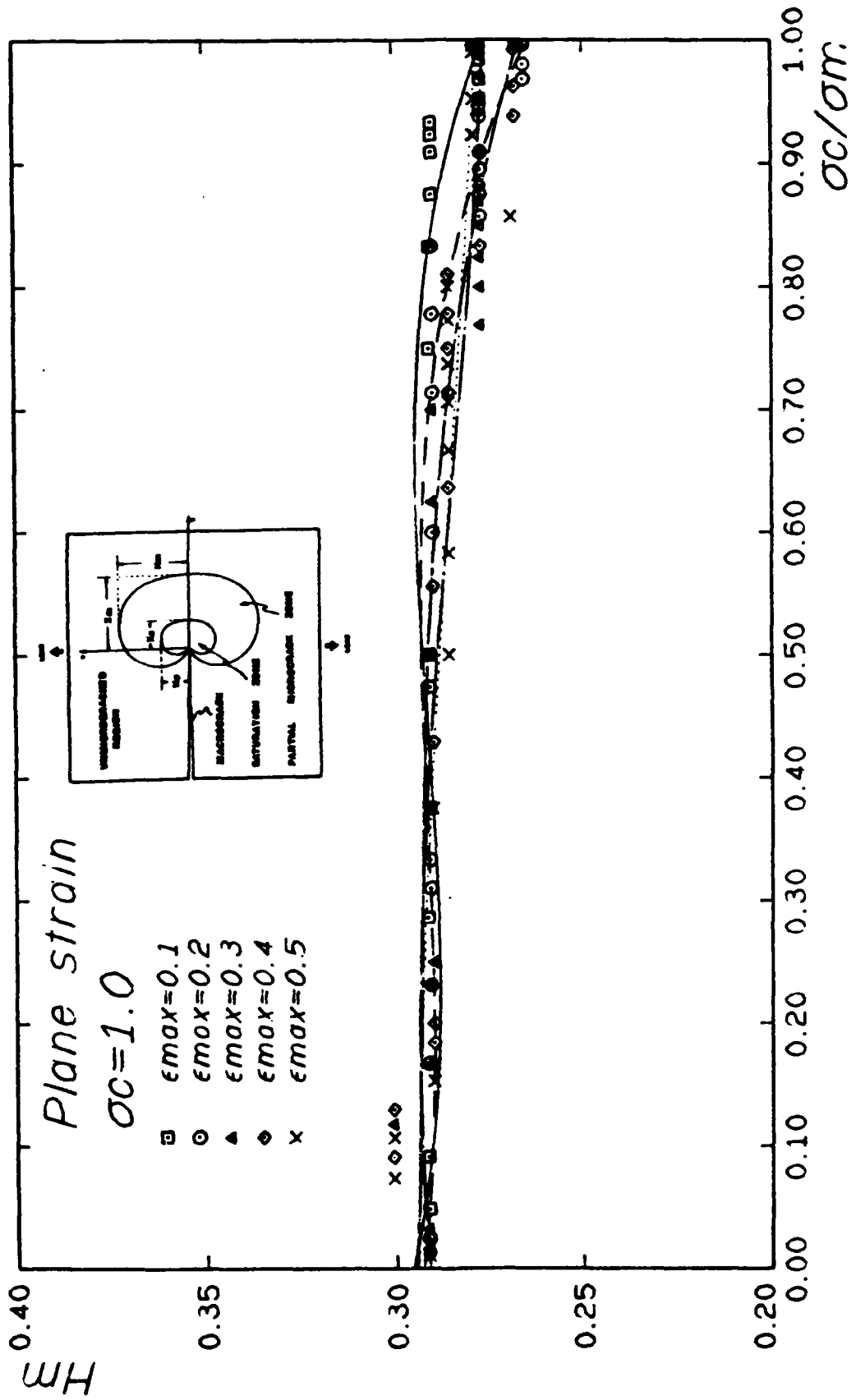


Fig. 9  $H_m$  maximum height of microcracked zone

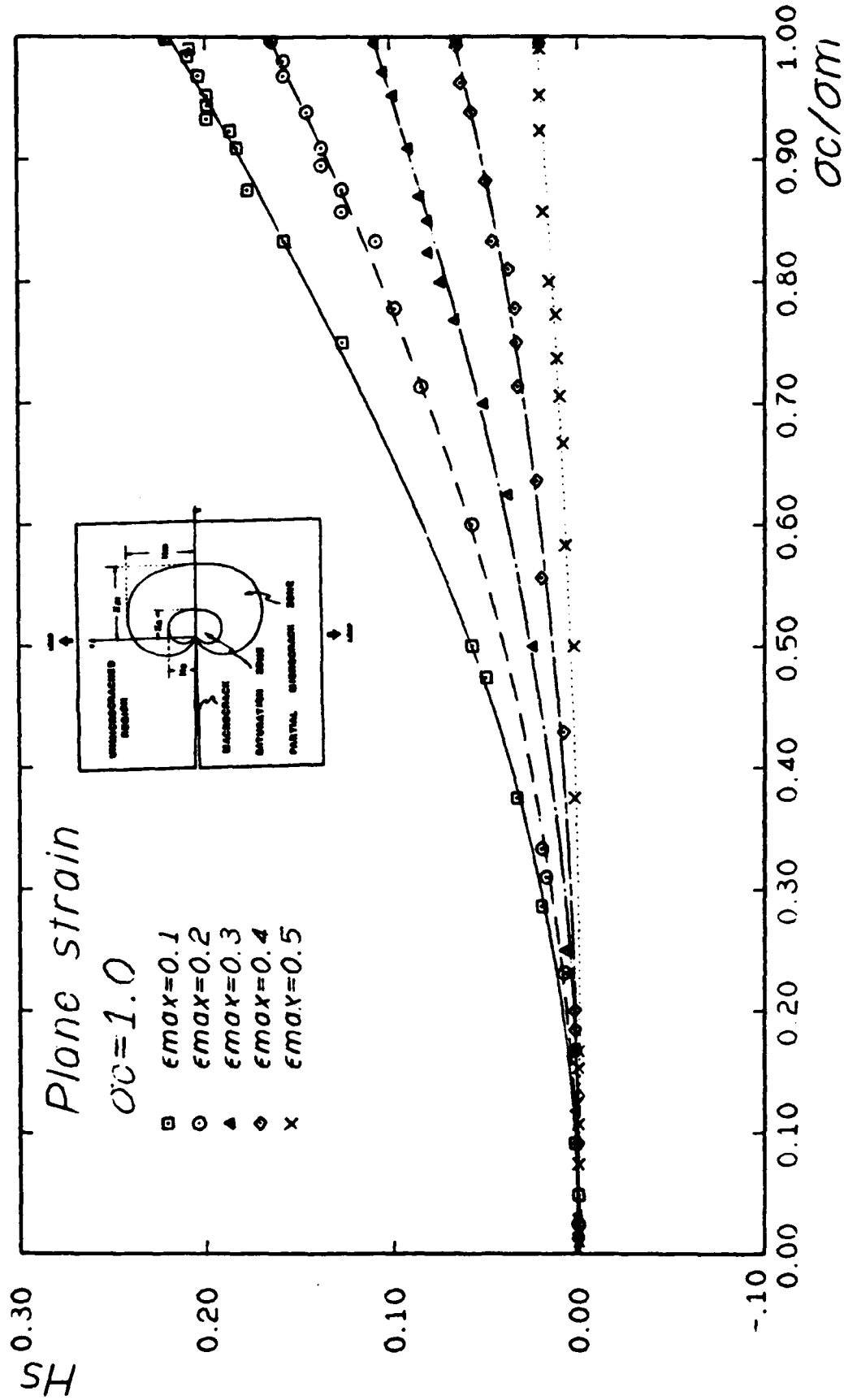


Fig. 90  $H_s$  Maximum height of saturated zone

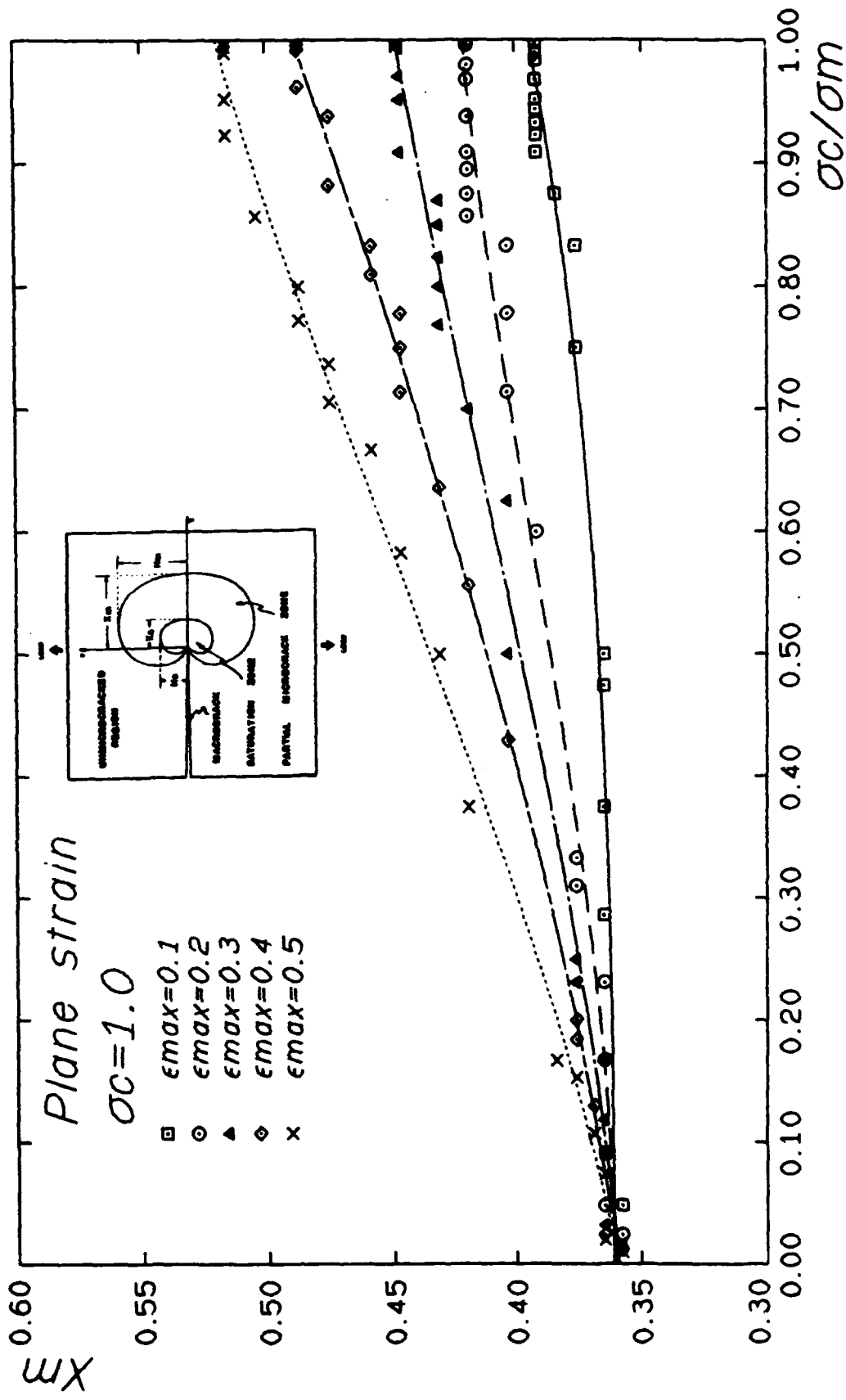


Fig. 9β  $X_m$  Maximum length of microcracked zone

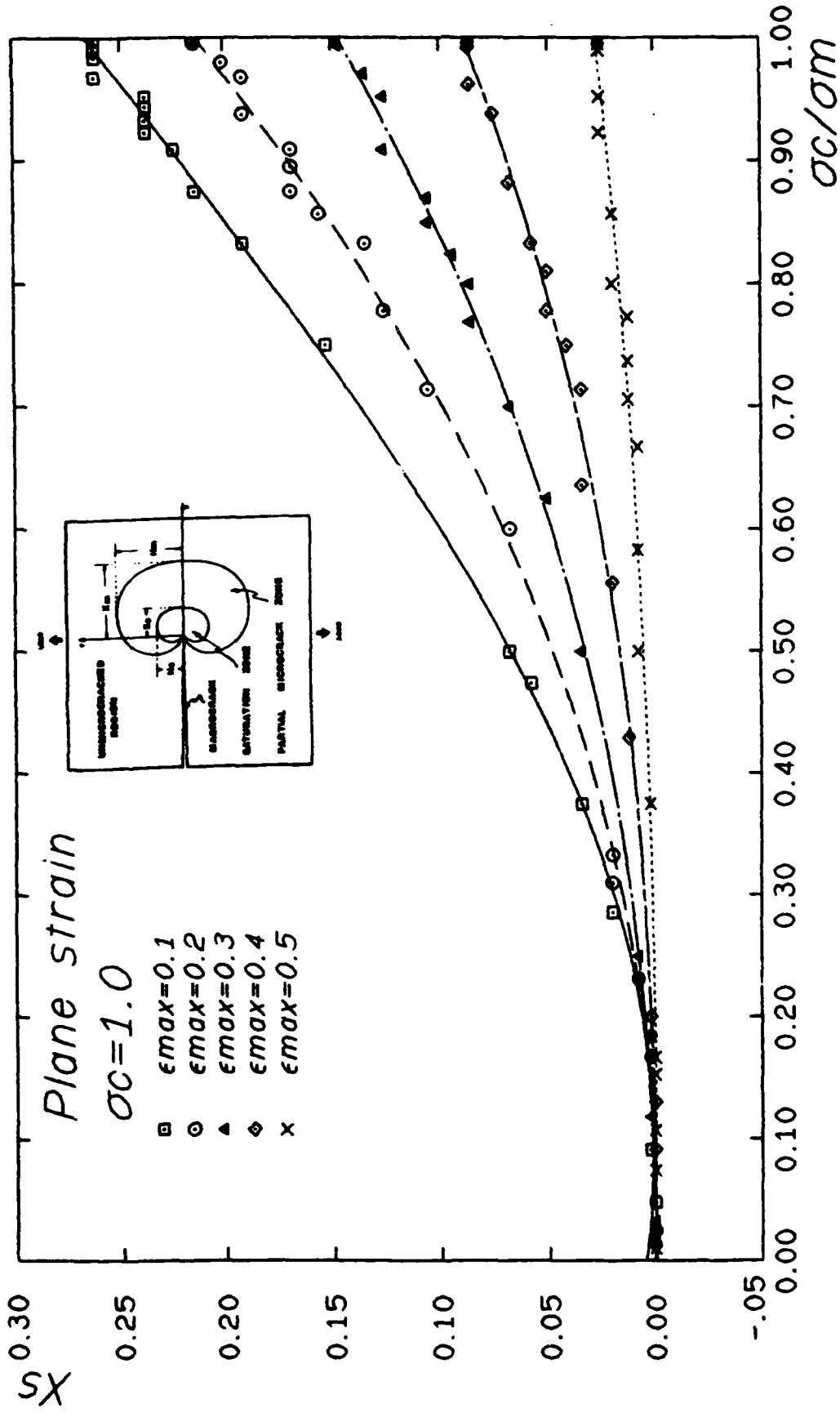


Fig. 97  $s_x$  Maximum length of saturated zone

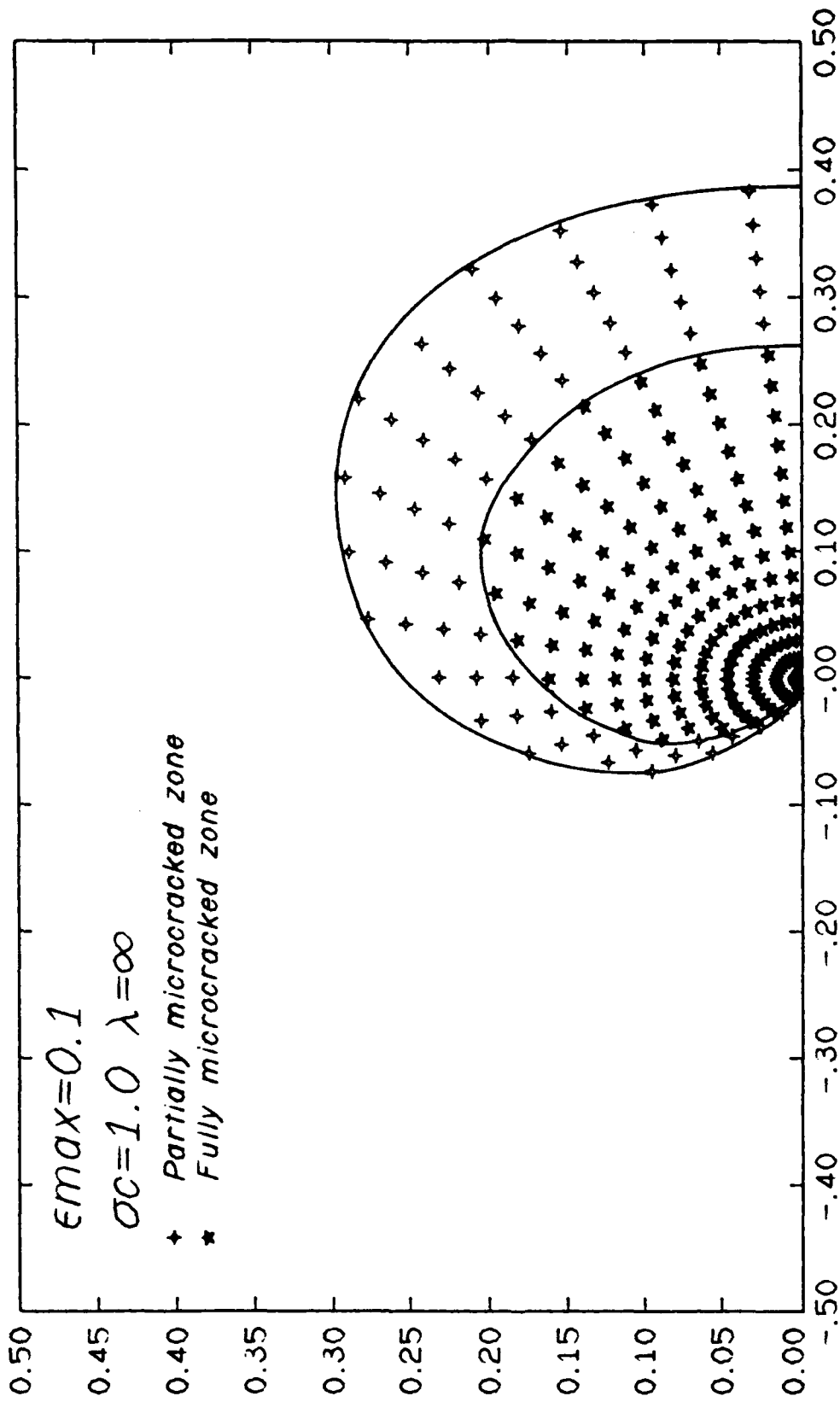


Fig. 10 The transformation zone around the crack tip

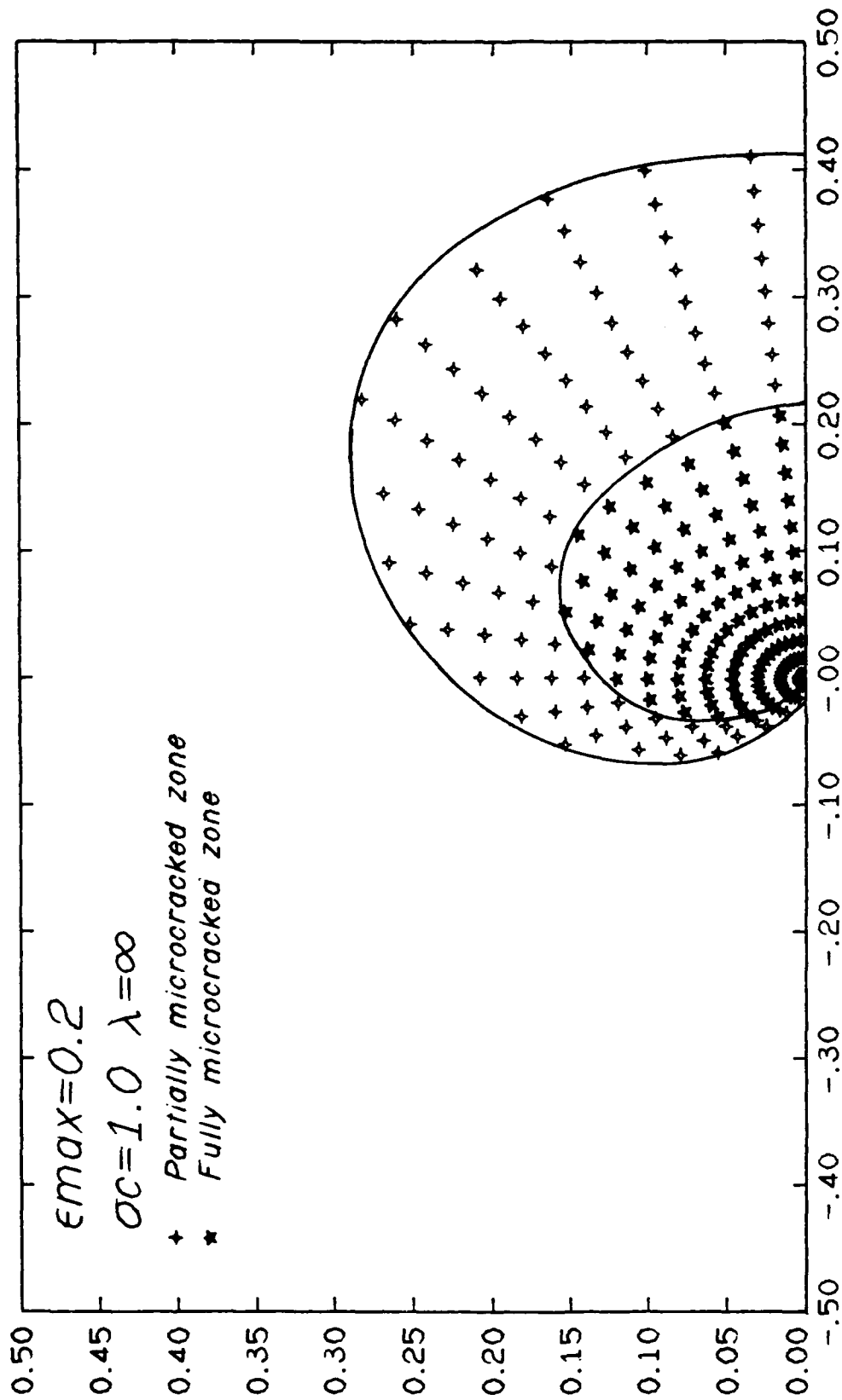


Fig. 10β The transformation zone around the crack tip

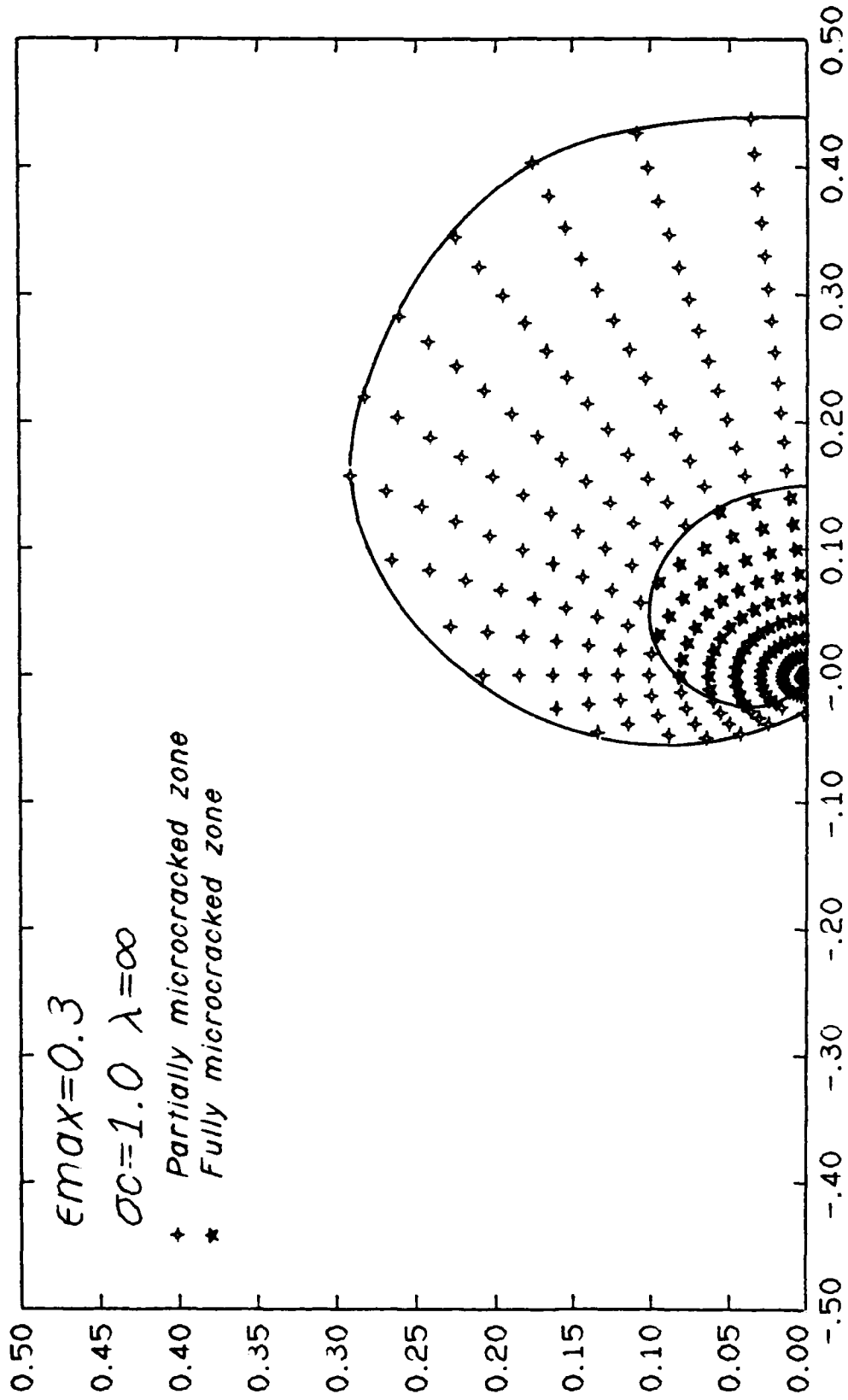


Fig. 10γ The transformation zone around the crack tip

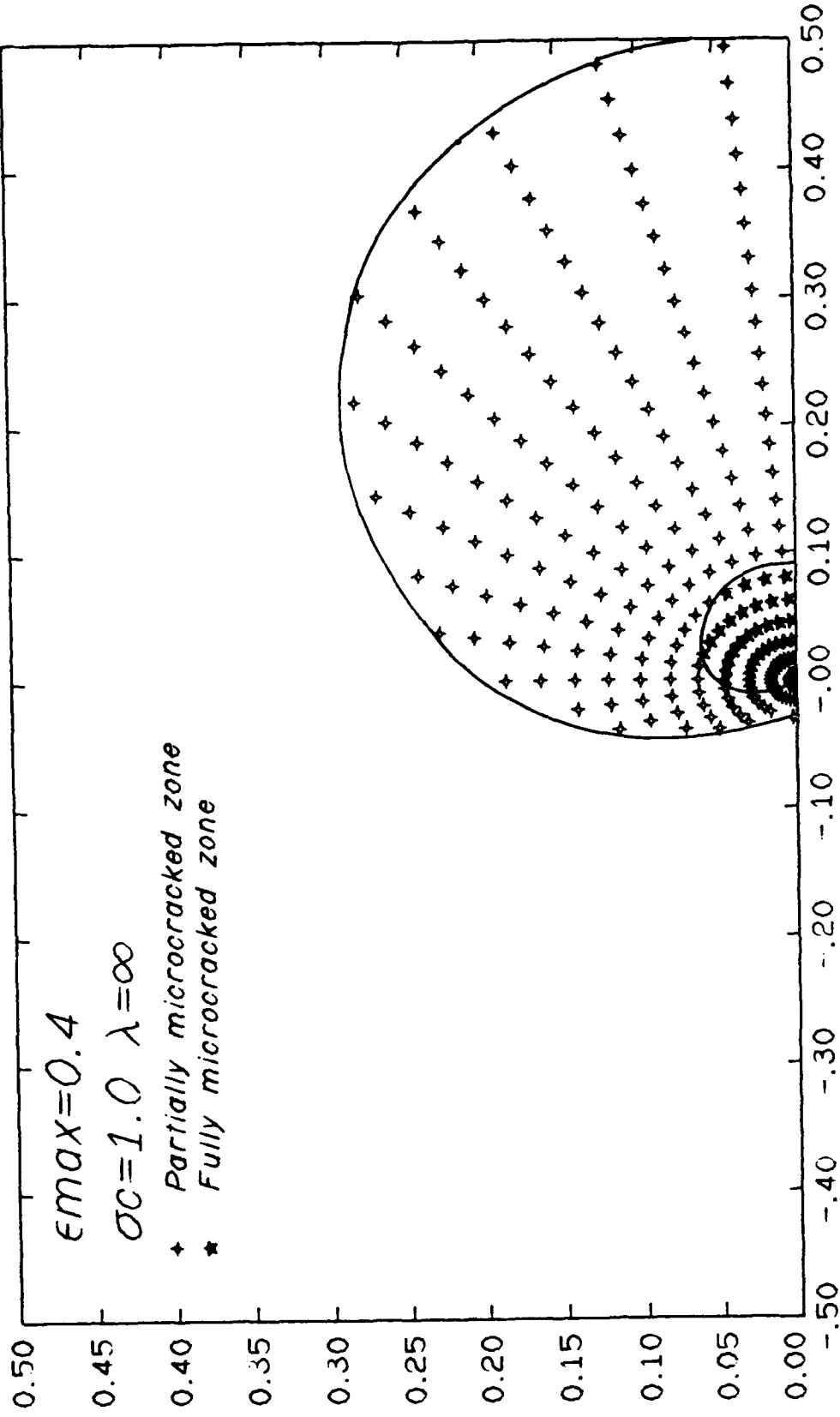


Fig. 106 The transformation zone around the crack tip

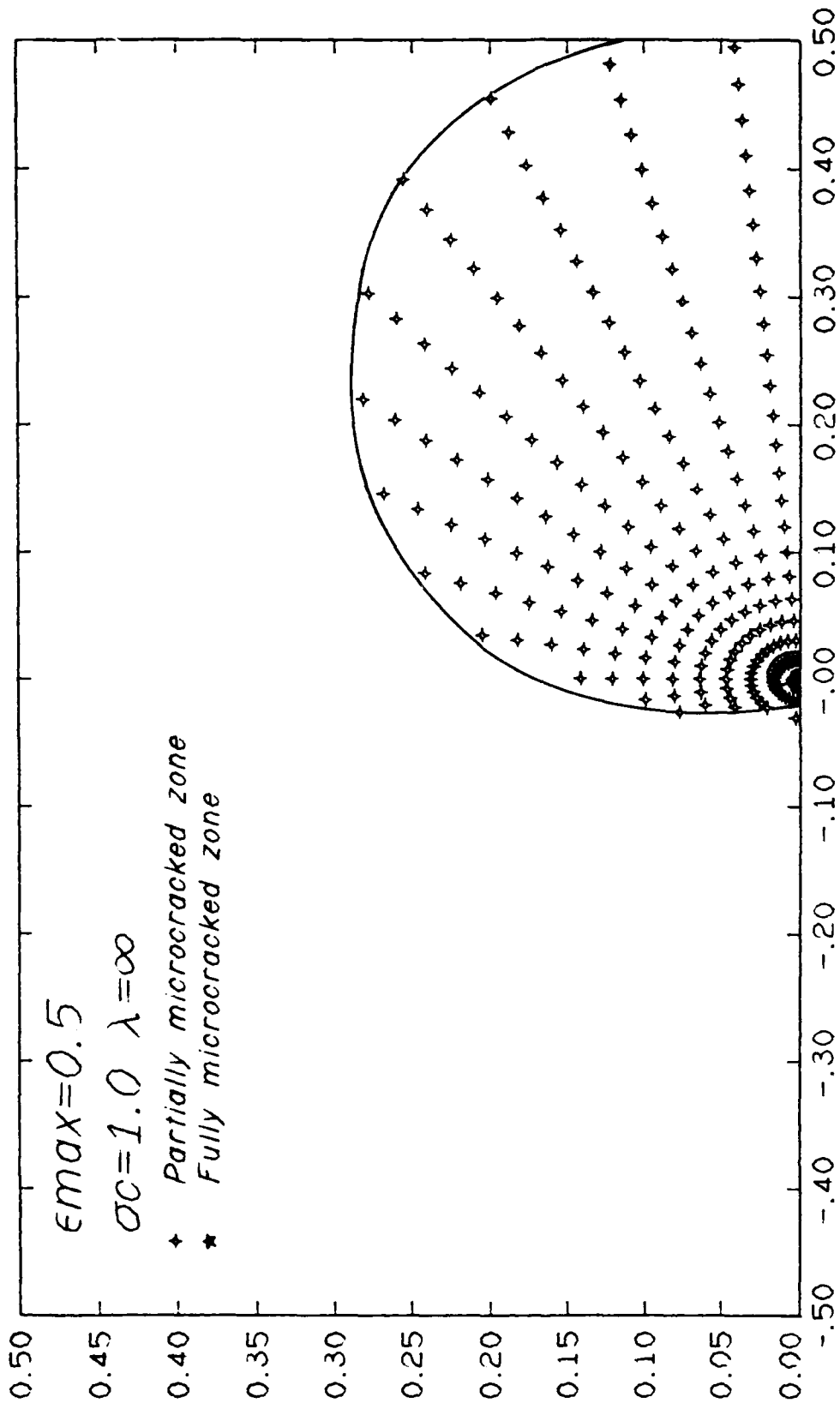


Fig. 10e The transformation zone around the crack tip

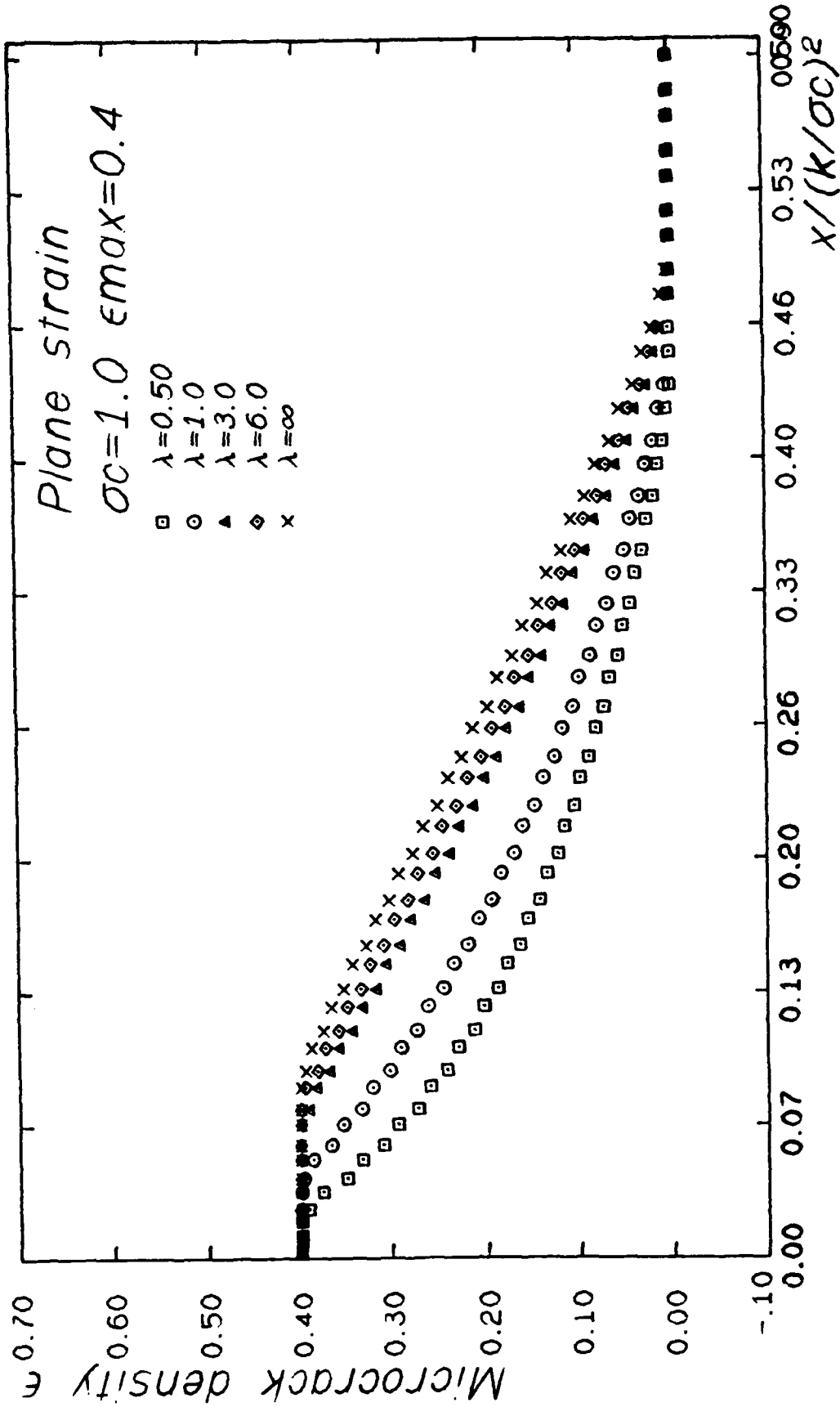


Fig. 11 Microcrack density ahead of the crack tip

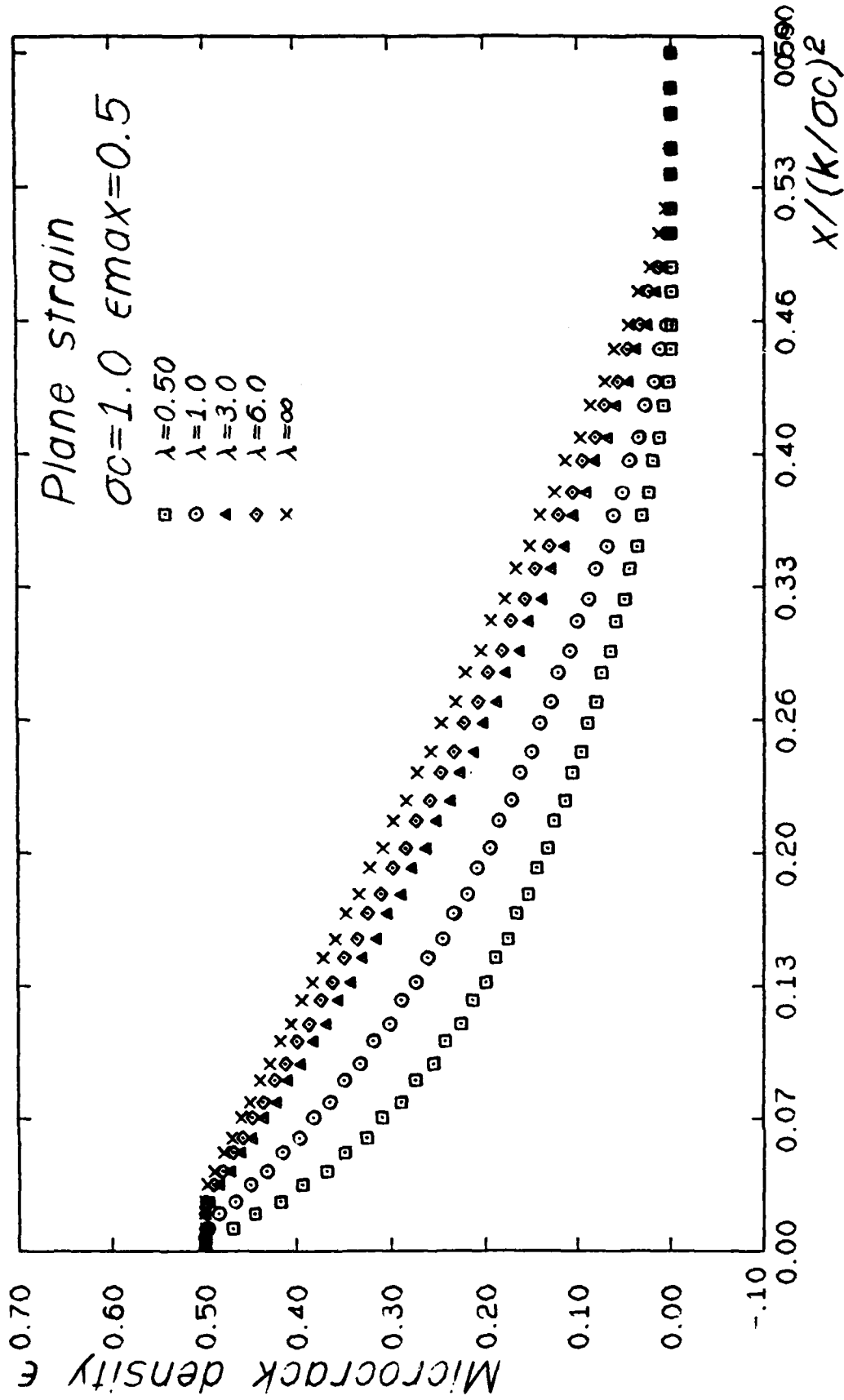


Fig. 12 Microcrack density ahead of the crack tip

**END**

**FILMED**

**7-85**

**DTIC**